2026

15 Degree pipe bend FEM Report

HYDROFOAMER

PETER RUPERT – CAE WORK

Table of Contents

List of figures

Units

Units are in Metric standard.

Unit System	Metric (mm, kg, N, s, mV, mA) Degrees rad/s Celsius
Angle	Degrees
Rotational Velocity	rad/s
Temperature	Celsius

Foreword

This numerical analysis has been undertaken to assess the global structural behavior of a DN800 buried pipeline incorporating a 15° bend section encapsulated in a foam support system and surrounded by in-situ soil.

The study has been developed to better understand the overall deformation response of the pipeline under operational loading, with particular attention given to the interaction between the bend, the adjacent straight pipe sections, the coupler, and the surrounding foam–soil system.

The simulation is intended to provide engineering insight into load transfer mechanisms, deformation trends, and restraint performance of the foam block, thereby supporting design evaluation and risk assessment during installation and service conditions.

The results are not intended to represent detailed sealing performance or micro-scale gasket behavior, but rather to capture the primary structural response of the pipeline system as a whole.

Scope

The primary objectives of this analysis are:

- To determine the global deformation behaviour of the pipeline system, with emphasis on the 15° bend region.
- To quantify pipe displacement and misalignment within the coupler, specifically at the interface between the straight pipe segment and the bend pipe segment.
- To evaluate the effectiveness of the foam encapsulation in restraining the pipeline and distributing thrust loads into the surrounding soil.
- To understand how loads are transferred from the pipe into the foam and subsequently into the soil.

This simulation focuses on total pipe deformation and structural response, rather than detailed local behaviour within sealing components.

The scope includes:

- Global structural deformation of the pipeline, including:
    - Bend region response
    - Straight-to-bend transition behaviour
    - Pipe misalignment and displacement within the coupler
- Interaction between:
    - Pipe and foam
    - Foam and surrounding soil
- Assessment of foam restraint effectiveness in maintaining pipe position and stability
- Evaluation of stresses, reaction forces, and overall deformation patterns relevant to system performance

The following aspects are **not** included in the present scope:

- Detailed evaluation of seal geometry, seal contact behaviour, and sealing performance
- Localized deformation and stress analysis within the gasket material
- Leakage performance, sealing pressure distribution, or fluid-tightness assessment
- Fine-scale contact modelling of seal lips or micro-level interface behaviour

The seal has been simplified and modelled as a block-shaped component with assigned elastic properties to approximate its flexibility and influence on the structural response.

In real-life application, the exact seal shape, material behaviour, and sealing function require separate detailed investigation and experimental validation, which are beyond the scope of this study.

This ensures that the analysis remains focused on the mechanical deformation and allows simulations to be executed fairly efficient manner, without capturing the seals detailed, difficult geometry and non-linear behaviour

Part geometry

The numerical model comprises the in-situ soil, backfill material, foam encapsulation, straight pipe sections, a pipe bend, a coupler, and two gaskets. To improve computational efficiency while preserving the physical behavior of the system, only one half of the geometry is modelled. Accordingly, the pipe bend is represented as a 7.5° segment, with a symmetry boundary condition applied at the mid-plane. This symmetry condition ensures that the model accurately represents the full 15° bend configuration, allowing the complete structural response to be captured while reducing model size and solution time. Appendix 4 shows a drawing of the geometry with the dimensions.

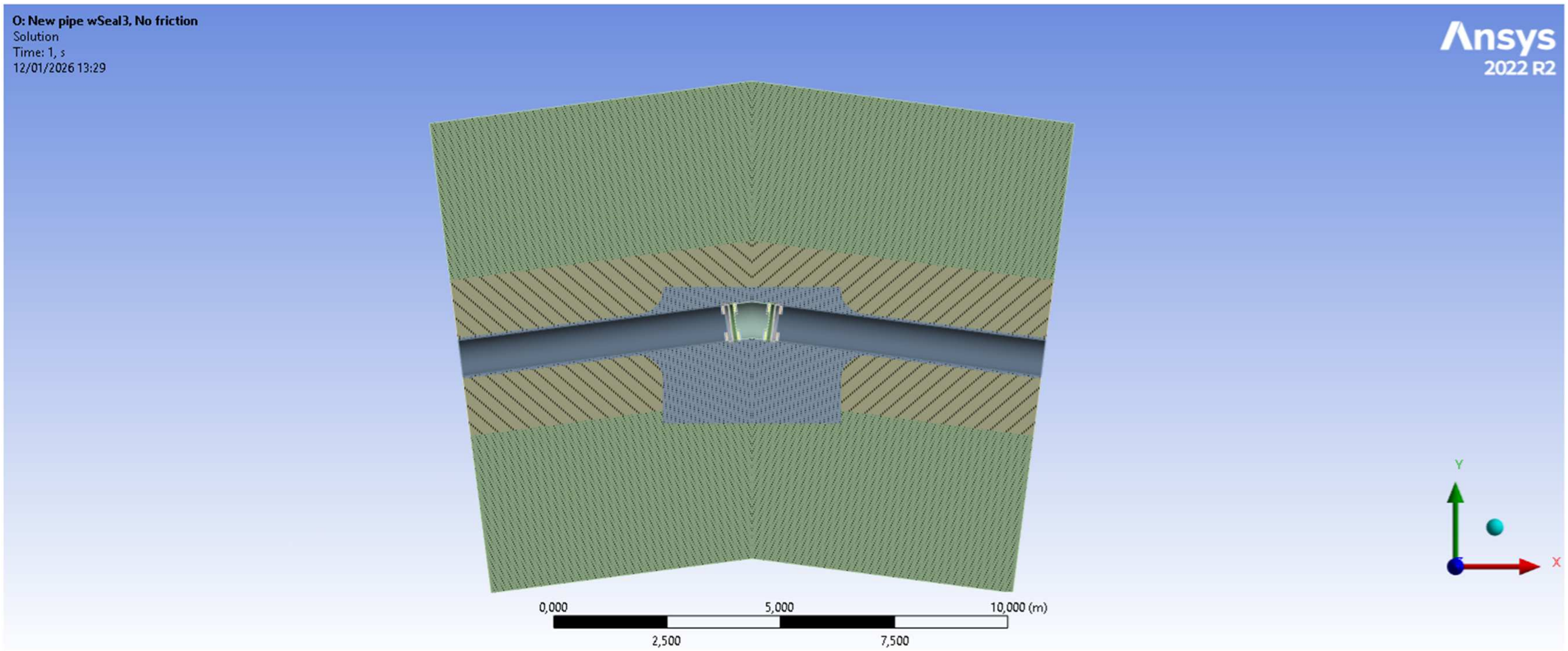

Figure 1 Part geometry

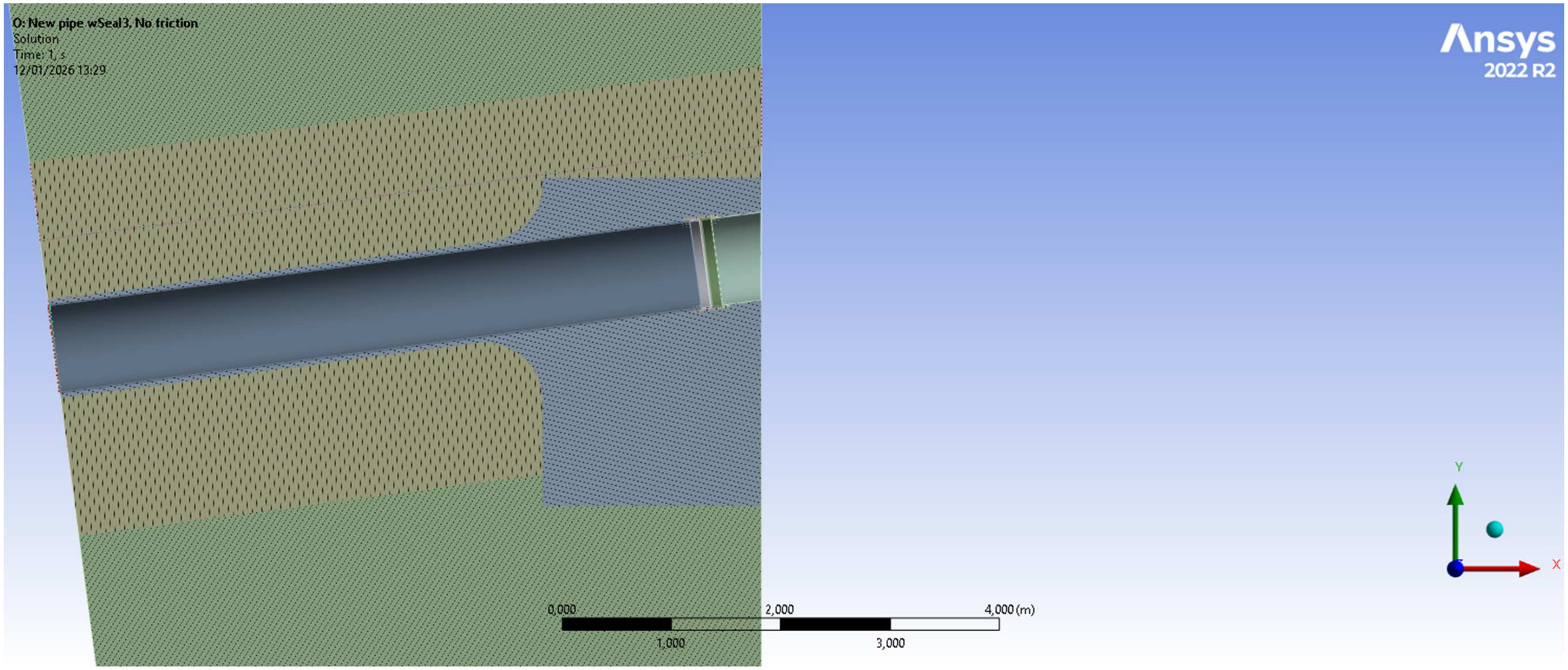

Figure 2 Geometry (half)

<table>
<tr><td>Object Name</td><td>Coupler</td><td>Foam</td><td>InSituSoil</td><td>RubberSeal</td><td>PipeCorner1</td><td>RubberSeal2</td><td>Pipe2</td><td>Backfill</td><td>Pipe</td><td>PipeCorner2</td></tr>
<tr><td>State</td><td colspan="3">Hidden</td><td>Meshed</td><td>Hidden</td><td>Meshed</td><td colspan="4">Hidden</td></tr>
<tr><td colspan="11">Graphics Properties</td></tr>
<tr><td>Visible</td><td colspan="3">No</td><td>Yes</td><td>No</td><td>Yes</td><td colspan="4">No</td></tr>
<tr><td>Glow</td><td colspan="10">0</td></tr>
<tr><td>Shininess</td><td colspan="10">1</td></tr>
<tr><td>Transparency</td><td colspan="10">1</td></tr>
</table>

Specularity	1									
Definition										
Suppressed	No									
ID (Beta)	34	37	40	43	46	49	52	109	1247	1250
Stiffness Behavior	Flexible									
Coordinate System	Pipe Coordinate System	Default Coordinate System		Pipe Coordinate System				Default Coordinate System	Pipe Coordinate System	
Reference Temperature	By Environment									
Treatment	None									
Material										
Assignment	Composite Pipe	PU Foam	In-situ Sand Soil	Rubber, nitrile (NBR) iso linear	Composite Pipe	Rubber, nitrile (NBR) iso linear	Composite Pipe	Sand Soil Backfill	Composite Pipe	
Nonlinear Effects	Yes		No		Yes	No	Yes			
Thermal Strain Effects	Yes			No	Yes	No	Yes			

Bounding Box										
Length X	441,61 mm	6519,1 mm	7140,4 mm	135,5 mm	460,31 mm	135,5 mm	196,35 mm	7075,2 mm	5966,9 mm	196,35 mm
Length Y	912,27 mm	3000, mm	11274 mm	853,89 mm	875,57 mm	853,89 mm	826,69 mm	10273 mm	1586,4 mm	826,69 mm
Length Z	876,7 mm	1422, mm	4712, mm	861,26 mm	822, mm	861,26 mm	822, mm	3711, mm	822, mm	
Properties										
Volume	1,7721e+007 mm³	9,2701e+009 mm³	1,8052e+011 mm³	1,1297e+006 mm³	1,1495e+007 mm³	1,1297e+006 mm³	2,5174e+006 mm³	1,2665e+011 mm³	1,6564e+008 mm³	2,5174e+006 mm³
Mass	36,984 kg	482,05 kg	3,4299e+005 kg	1,1121 kg	23,991 kg	1,1121 kg	5,2538 kg	2,4064e+005 kg	345,69 kg	5,2538 kg
Centroid X	-503,65 mm	-1604,1 mm	-3264, mm	-621,95 mm	-204,76 mm	-385,35 mm	-556,11 mm	-3331,5 mm	-3530,4 mm	-451,19 mm
Centroid Y	-66,307 mm	-814, mm	-150,28 mm	-81,882 mm	3,4124e-002 mm	-50,733 mm	-73,214 mm	-326,91 mm	-464,79 mm	-59,401 mm
Centroid Z	-2,2381e-006 mm	-66,642 mm	-38,712 mm	6,0358e-006 mm	-3,1216 mm	-4,7327e-007 mm	1,2648e-006 mm	1687,6 mm	-1,9509e-008 mm	2,9493e-006 mm
Moment of Inertia Ip1	6,7023e+006 kg·mm²	4,0049e+008 kg·mm²	4,9719e+012 kg·mm²	1,9471e+005 kg·mm²	3,9014e+006 kg·mm²	1,9471e+005 kg·mm²	8,6398e+005 kg·mm²	1,2306e+012 kg·mm²	5,6278e+007 kg·mm²	8,6398e+005 kg·mm²
Moment of Inertia Ip2	3,6626e+006 kg·mm²	1,1153e+009 kg·mm²	1,71e+012 kg·mm²	97406 kg·mm²	2,2788e+006 kg·mm²	97406 kg·mm²	4,3554e+005 kg·mm²	1,0069e+012 kg·mm²	1,0293e+009 kg·mm²	4,3554e+005 kg·mm²
Moment of Inertia Ip3	3,6626e+006 kg·mm²	1,3475e+009 kg·mm²	5,7036e+012 kg·mm²	97406 kg·mm²	2,3054e+006 kg·mm²	97406 kg·mm²	4,3554e+005 kg·mm²	1,8458e+012 kg·mm²	1,0293e+009 kg·mm²	4,3554e+005 kg·mm²
Statistics										
Nodes	121758	414472	199776	1140	32160	1140	6060	265464	198660	6060
Elements	69326	266510	138186	120	6300	120	1080	181823	39600	1080
Mesh Metric	None									

Pre-processing / boundary conditions

Boundary constraints consist of fixed supports applied to the bottom and lateral faces of the in-situ soil domain, while the external open boundaries of the model are restrained in the global X-direction (0 X-displacement) to prevent rigid body motion. In addition, a symmetry boundary condition is enforced at the mid-plane of the 15° bend, enabling efficient simulation of the system while preserving the physical response of the full geometry.

Symmetry boundary condition

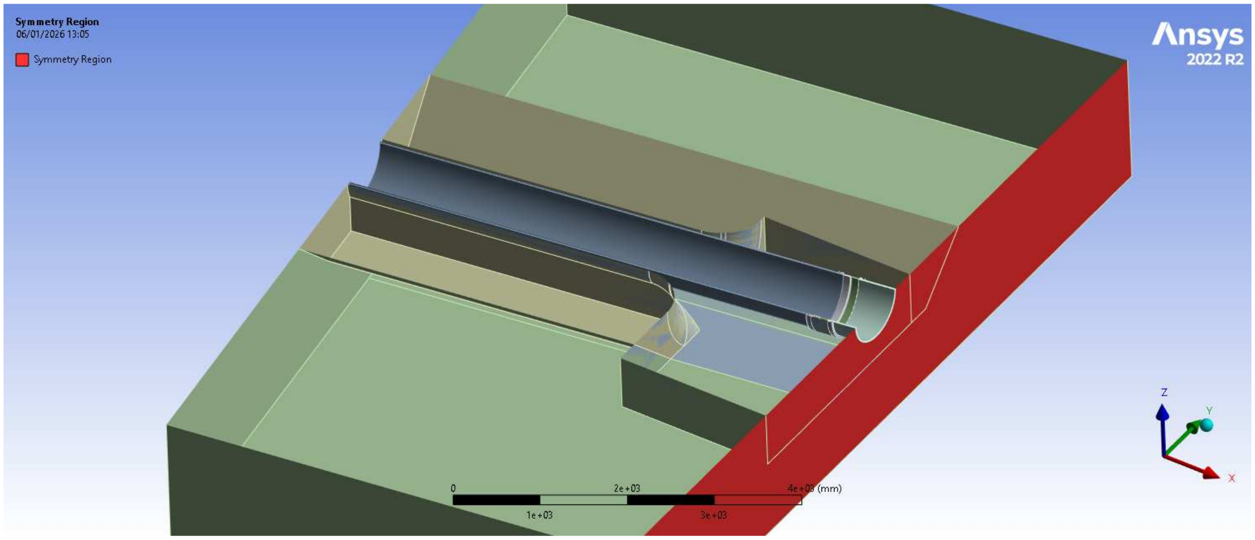

Figure 3 Symmetry boundary condition

Object Name	*Symmetry*
State	Fully Defined
Graphical Expansion 1 (Beta)	
Num Repeat	2
Type	Cartesian
Method	Half
ΔX	0,1 mm
ΔY	0, mm
ΔZ	0, mm
Coordinate System	Global Coordinate System

Object Name	*Symmetry Region*
State	Fully Defined
Scope	
Scoping Method	Geometry Selection
Geometry	5 Faces
Definition	
Scope Mode	Manual
Type	Symmetric
Coordinate System	Global Coordinate System
Symmetry Normal	X Axis
Suppressed	No

Standard earth gravity boundary condition

Object Name	*Standard Earth Gravity*
State	Fully Defined
Scope	
Geometry	All Bodies
Definition	
Coordinate System	Global Coordinate System
X Component	0, mm/s² (ramped)
Y Component	0, mm/s² (ramped)
Z Component	-9806,6 mm/s² (ramped)
Suppressed	No
Direction	-Z Direction

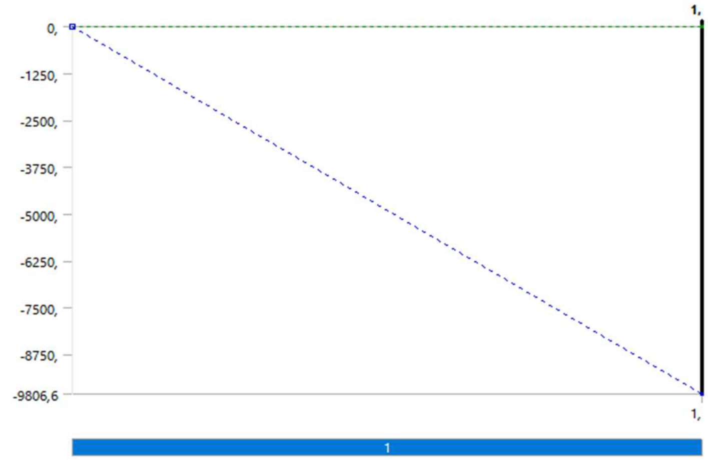

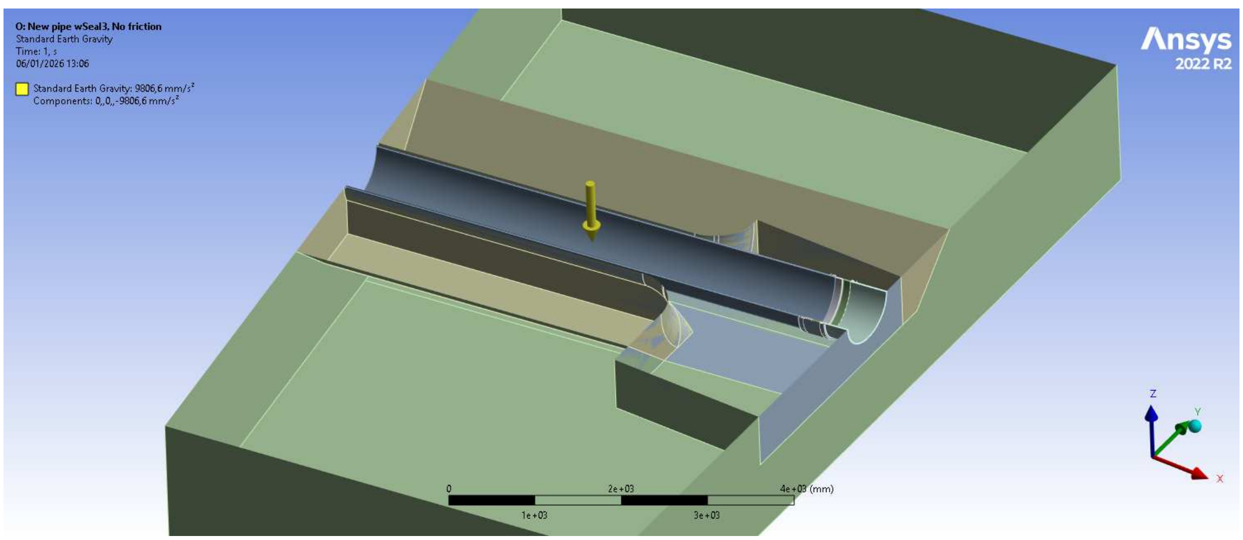

Figure 4 Standard earth gravity boundary condition

Load conditions

The numerical model incorporates all primary operational and environmental loads acting on the pipeline system. An internal pipe pressure of 1.52 MPa is applied uniformly to the internal pipe surface. External hydrostatic pressure is applied from the pipe bottom surface up, with the free surface condition at the top of the pipe inner surface. Gravity loading is included for all components of the model to account for self-weight effects.

Summary

Object Name	*Hydrostatic Pressure 2*	*Fixed Support*	*Displacement*	*Pressure*
State	Fully Defined			
Scope				
Scoping Method	Geometry Selection			
Geometry	16 Faces	4 Faces	5 Faces	13 Faces
Definition				
ID (Beta)	576	586	645	1063
Type	Hydrostatic Pressure	Fixed Support	Displacement	Pressure
Applied By	Surface Effect			Surface Effect
Coordinate System	Global Coordinate System		EndSectionCoordinate System	
Fluid Density	9,97e-007 kg/mm³			
Suppressed	No			
Define By			Components	Normal To
X Component			0, mm (ramped)	
Y Component			Free	
Z Component			Free	
Loaded Area				Deformed
Magnitude				1,52 MPa (ramped)
Hydrostatic Acceleration				
Define By	Components			

Hydrostatic pressure

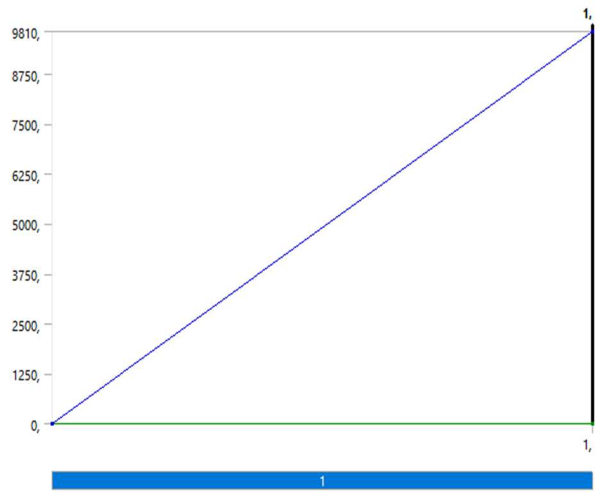

X-displacement fixture

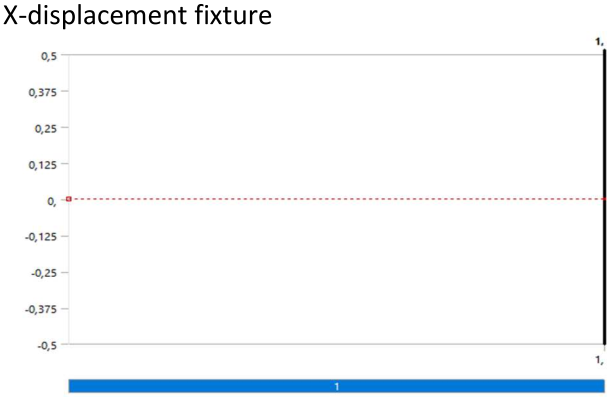

X Component	0, mm/s² (ramped)	
Y Component	0, mm/s² (ramped)	
Z Component	9810, mm/s² (ramped)	
Free Surface Location		
X Coordinate	0, mm	
Y Coordinate	0, mm	
Z Coordinate	400, mm	
Location	Defined	

Internal pipe pressure

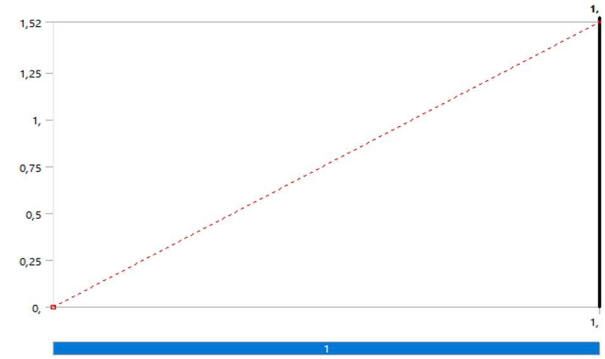

Hydrostatic pressure

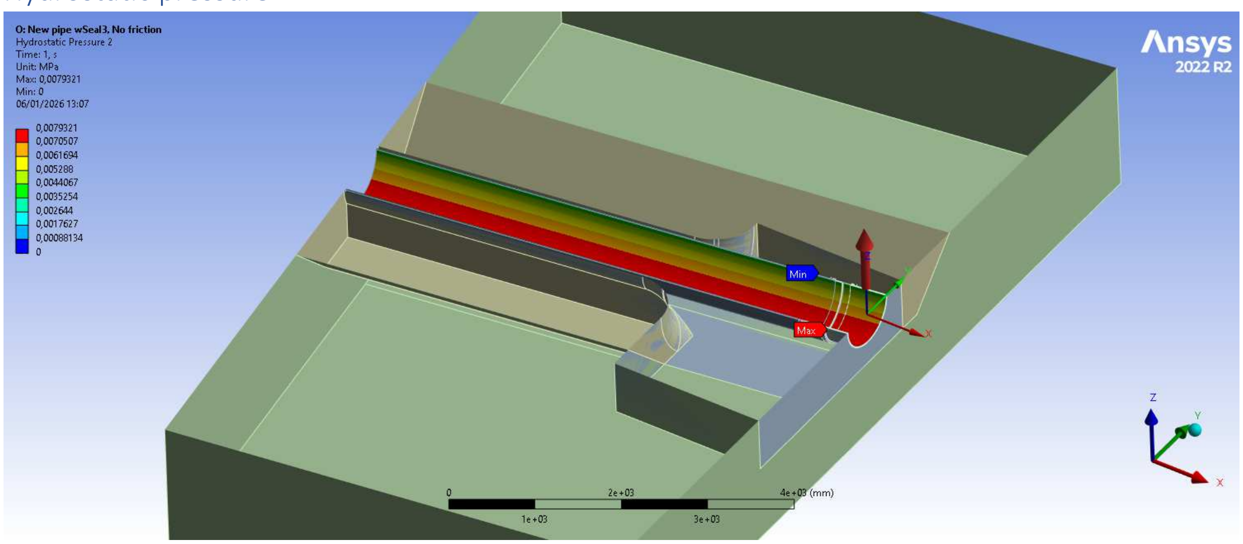

Figure 5 Hydrostatic pressure load condition

External fixture

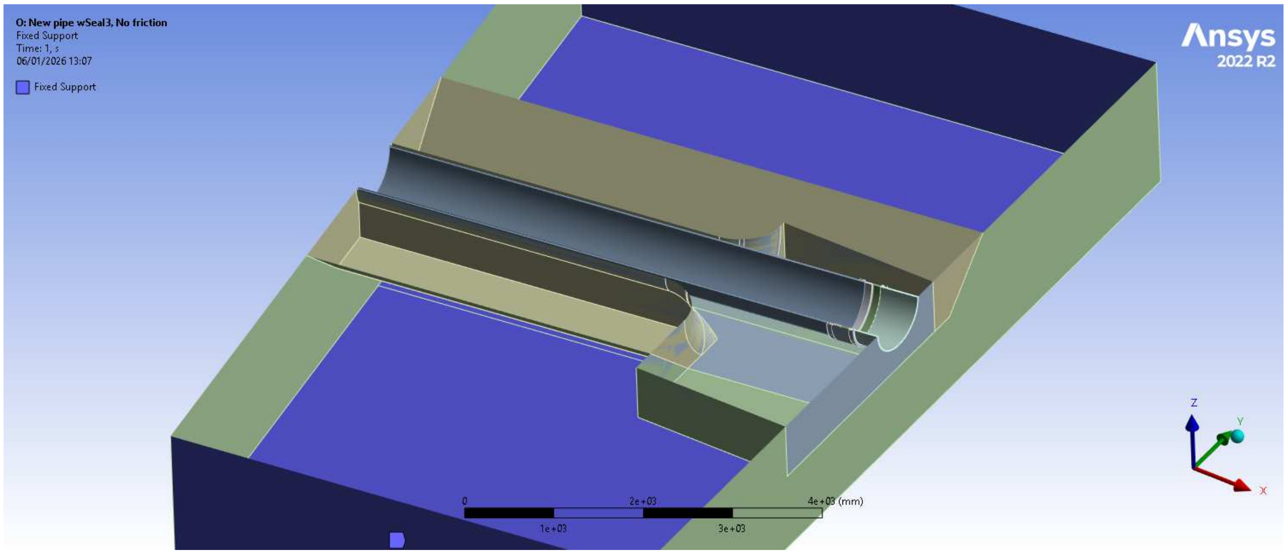

Figure 6 External fixture boundary condition

0 X-displacement

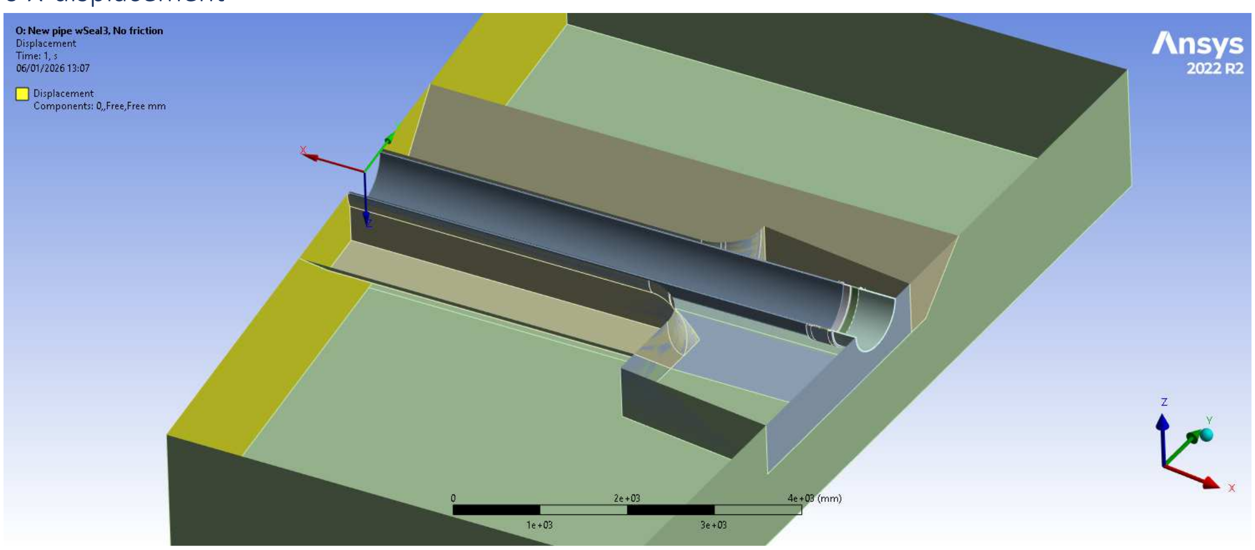

Figure 7 0 x-direction displacement (end condition)

Internal pipe pressure

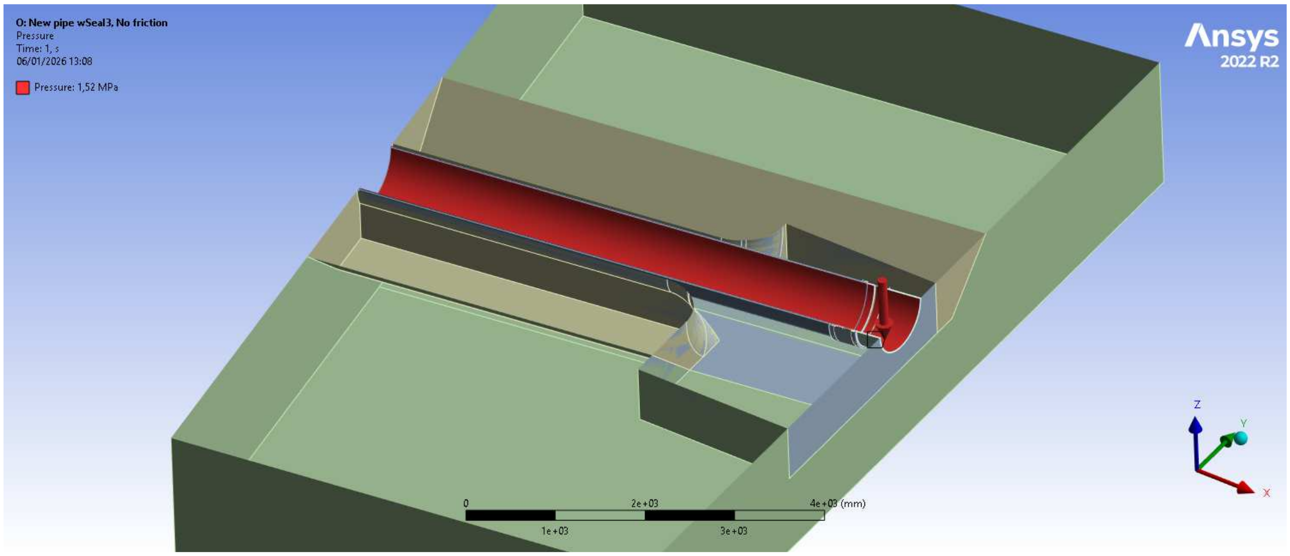

Figure 8 Internal pipe pressure load condition

Material mechanical properties

Material overview	Composite Pipe		CZM failure		Rubber, nitrile (NBR)		Rubber, nitrile (NBR) iso linear		In-situ Sand Soil		PU Foam		Sand Soil Backfill	
Density	2.09E-03	kg/mm³	FAILURE CRITERION		9.84E-04	kg/mm³	9.84E-04	kg/mm³	1.90E-06	kg/mm³	5.20E-08	kg/mm³	1.90E-06	kg/mm³
Isotropic Elasticity														
Derive from							Young's Modulus and Poisson's Ratio		Young's Modulus and Poisson's Ratio		Young's Modulus and Poisson's Ratio		Young's Modulus and Poisson's Ratio	
Young's Modulus							4	MPa	200	MPa	4	MPa	70	MPa
Poisson's Ratio							0.35		0.3		0.3		0.25	
Bulk Modulus							4	MPa	166,67	MPa	3	MPa	47	MPa
Shear Modulus							1	MPa	77	MPa	1	MPa	28	MPa
Orthotropic Elasticity														
Young's Modulus X direction	2620	MPa												
Young's Modulus Y direction	13000	MPa												
Young's Modulus Z direction	26200	MPa												
Poisson's Ratio XY	0.2													
Poisson's Ratio YZ	0.2													
Poisson's Ratio XZ	0.2													
Shear Modulus XY	500	MPa												
Shear Modulus YZ	1000	MPa												
Shear Modulus XZ	10300	MPa												
Orthotropic Stress Limits														
Tensile X direction	20	MPa												
Tensile Y direction	200	MPa												
Tensile Z direction	250	MPa												

Compressive X direction	-30	MPa												
Compressive Y direction	-150	MPa												
Compressive Z direction	-200	MPa												
Shear XY	15	MPa												
Shear YZ	20	MPa												
Shear XZ	60	MPa												
Orthotropic Strain Limits														
Tensile X direction	0.015													
Tensile Y direction	0.02													
Tensile Z direction	0.03													
Compressive X direction	-0.02													
Compressive Y direction	-0.015													
Compressive Z direction	-0.02													
Shear XY	0.015													
Shear YZ	0.025													
Shear XZ	0.03													
Tsai-Wu Constants														
Coupling Coefficient XY	-1													
Coupling Coefficient YZ	-1													
Coupling Coefficient XZ	-1													
Tensile Ultimate Strength					5	MPa	5	MPa						
Tensile Yield Strength					5	MPa	5	MPa						

Uniaxial Test Data	Strain [Mm/Mm]	Stress [M Pa]
	0,030000	0,19900
	0,022500	0,14920
	0,015000	0,099500
	0,0075000	0,049700
	0	0
	-0,032200	-0,12500
	-0,024200	-0,093700
	-0,016100	-0,062500
	-0,0081000	-0,031400

Strain Hardening														
Reference Units (Length, Time, Temperature, Force)											mm, s, K, N			
Creep Constant 1											1.00E-12			
Creep Constant 2											10			
Creep Constant 3											0.2			
Creep Constant 4											0			
Mohr-Coulomb														
Yield Surface														
Initial Inner Friction Angle									38	degree			35	degree
Initial Cohesion									1	MPa			1	MPa
Dilatancy Angle									3	degree			0.6	degree
Residual Inner Friction Angle									35	degree			30	degree
Residual Cohesion									0.8	MPa			0.8	MPa

Fracture-Energies based Debonding														
Debonding Interface Mode			Mode II (Shear only)											
Tangential Slip Under Normal Compression			No											
Maximum Normal Contact Stress				MPa										
Critical Fracture Energy for Normal Separation				mJ/mm²										
Maximum Equivalent Tangential Contact Stress			0.10625	MPa										
Critical Fracture Energy for Tangential Slip			0.2	mJ/mm²										
Artificial Damping Coefficient			0	s										
Power Law Exponent for Mixed-Mode Debonding			20											

Contact definitions

Object Name	*Bonded - Backfill To InSituSoil*	*Bonded - Foam To Backfill*	*Bonded - InSituSoil To Foam*	*Bonded - Pipe To Foam*	*Bonded - PipeCorner1 To Foam*	*Bonded - Coupler To Foam*	*Bonded - RubberSeal To Pipe*	*Bonded - RubberSeal2 To PipeCorner1*	*Bonded - RubberSeal To Coupler*	*Bonded - RubberSeal2 To Coupler*	*Bonded - PipeCorner2 To PipeCorner1*
State	Fully Defined										
Scope											
Scoping Method	Geometry Selection										
Contact	4 Faces	15 Faces	5 Faces	2 Faces		3 Faces	2 Faces				
Target	4 Faces	15 Faces	3 Faces	1 Face		3 Faces	2 Faces		1 Face		2 Faces
Contact Bodies	Backfill	Foam	InSituSoil	Pipe	PipeCorner1	Coupler	RubberSeal	RubberSeal2	RubberSeal	RubberSeal2	PipeCorner2
Target Bodies	InSituSoil	Backfill	Foam				Pipe	PipeCorner1	Coupler		PipeCorner1
Protected	No										
Definition											
Type	Bonded										
Scope Mode	Manual										
Behavior	Program Controlled	Asymmetric	Program Controlled								
Trim Contact	Program Controlled										
Suppressed	No										
Object ID (Beta)	512	515	518	521	524	527	530	533	536	539	817
Display											
Element Normals	No										
Advanced											

Formulation	Program Controlled	Pure Penalty	Program Controlled	Pure Penalty	Program Controlled
Small Sliding	Program Controlled	On	Program Controlled		
Detection Method	Program Controlled				
Penetration Tolerance	Program Controlled				
Elastic Slip Tolerance	Program Controlled	Value	Program Controlled		
Normal Stiffness	Program Controlled	Factor	Program Controlled		
Update Stiffness	Program Controlled	Each Iteration	Program Controlled		
Pinball Region	Program Controlled				
Elastic Slip Tolerance Value		0,5 mm			
Normal Stiffness Factor		0,1			
Geometric Modification					
Contact Geometry Correction	None				
Target Geometry Correction	None				

Results

Simulation deformation tracker

A deformation tracker is placed at the apex vertex of the pipe bend to monitor displacement throughout the solution process. This tracking point is used to observe convergence behavior and verify the stability of the solution by ensuring that the pipe deformation reaches a steady value as the simulation progresses.

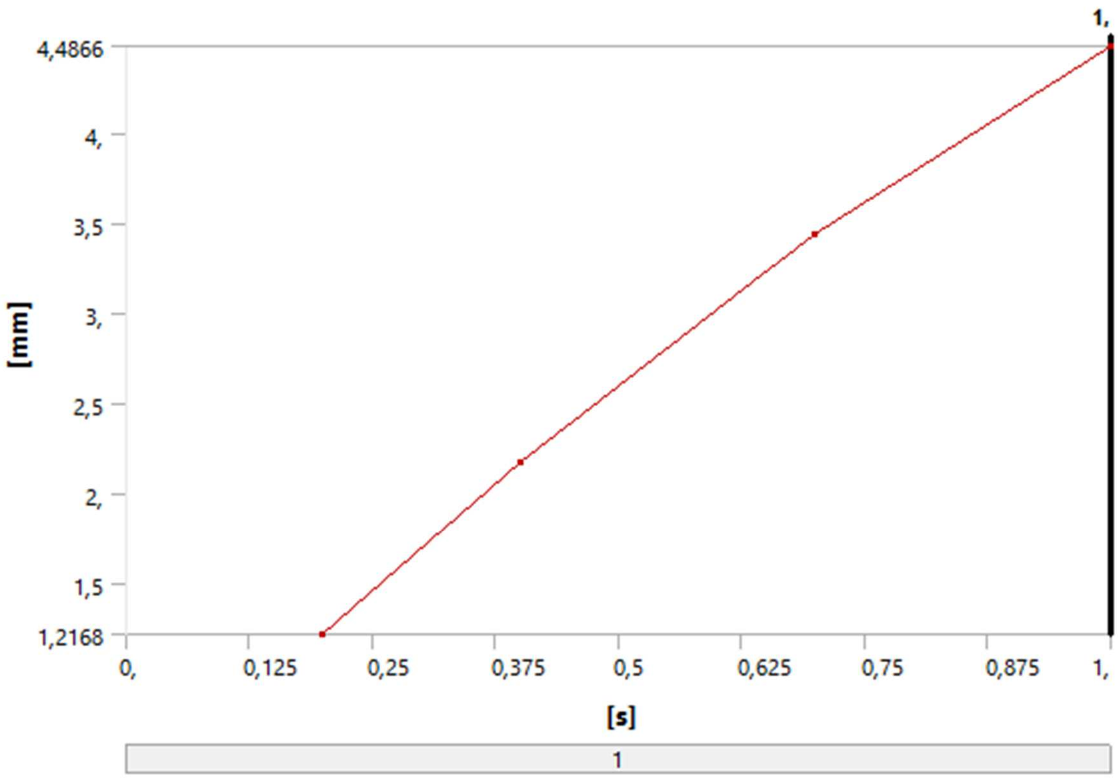

Figure 9 Deformation tracker at pipe apex

Total deformation results

A well distributed deformation of the pipe bend section is noticeable, the e-modulus of the gaskets (4MPa) are modelled with a slightly higher e-modulus compared to the compressive modulus (3.88MPa) of the foam, however they are within similar range. This results in a well distributed deformation, while higher deformation and displacements are measured near the apex of the bend.

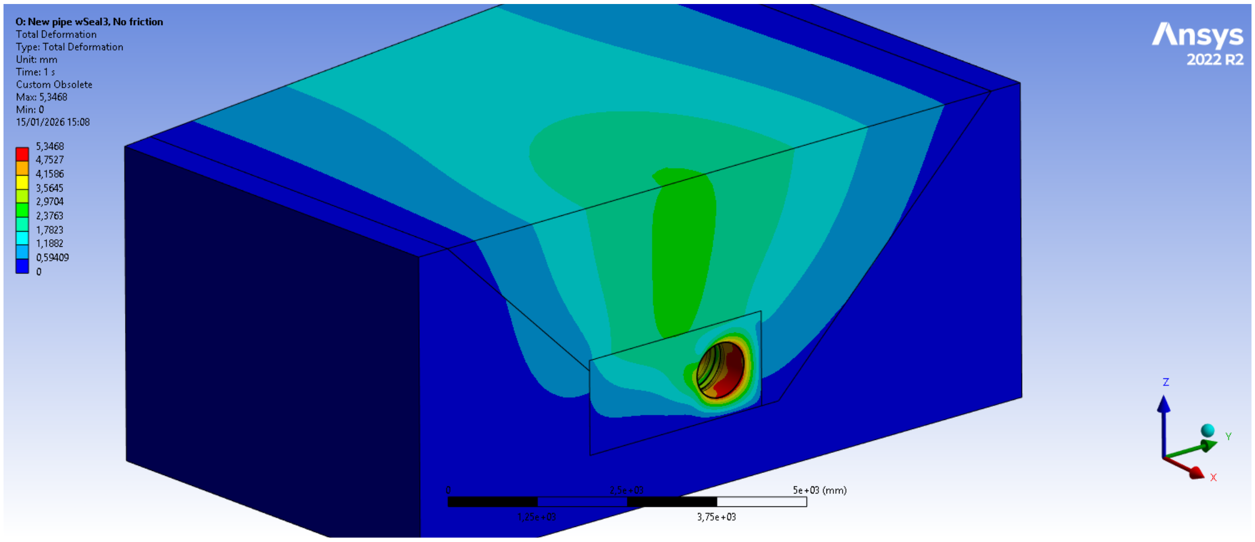

Figure 10 Total deformation of all bodies (half model)

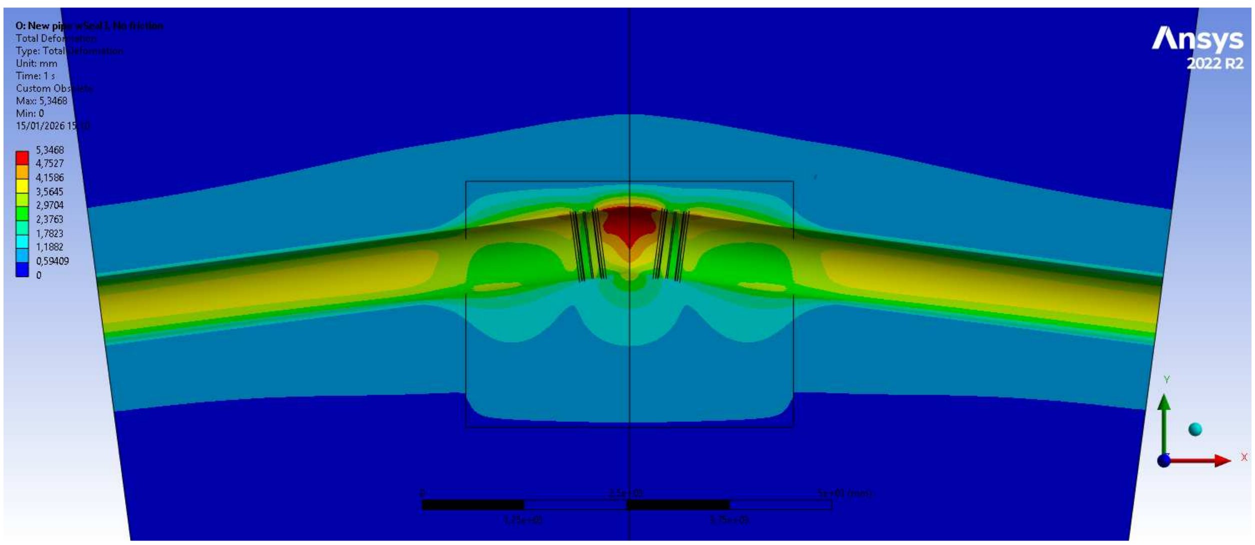

Figure 11 Cross-sectional view of the total deformation (full model)

Von-mises stress

The highest von Mises stresses are observed in the coupler region behind the gaskets, where the material is less elastic and therefore more sensitive to deformation. Increased pipe ovalization in this region leads to higher von Mises stress levels when compared to the rubber gasket, which is more compliant and able to accommodate deformation. Along the pipe body, the von Mises stress is generally well distributed and primarily governed by the applied internal pipe pressure, resulting in a relatively uniform stress pattern outside the coupler zone.

Due to the large contact surface area and the low elastic modulus of the foam material, the resulting von Mises stresses within the foam remain low, even while it effectively participates in restraining the pipeline and transferring loads to the surrounding soil.

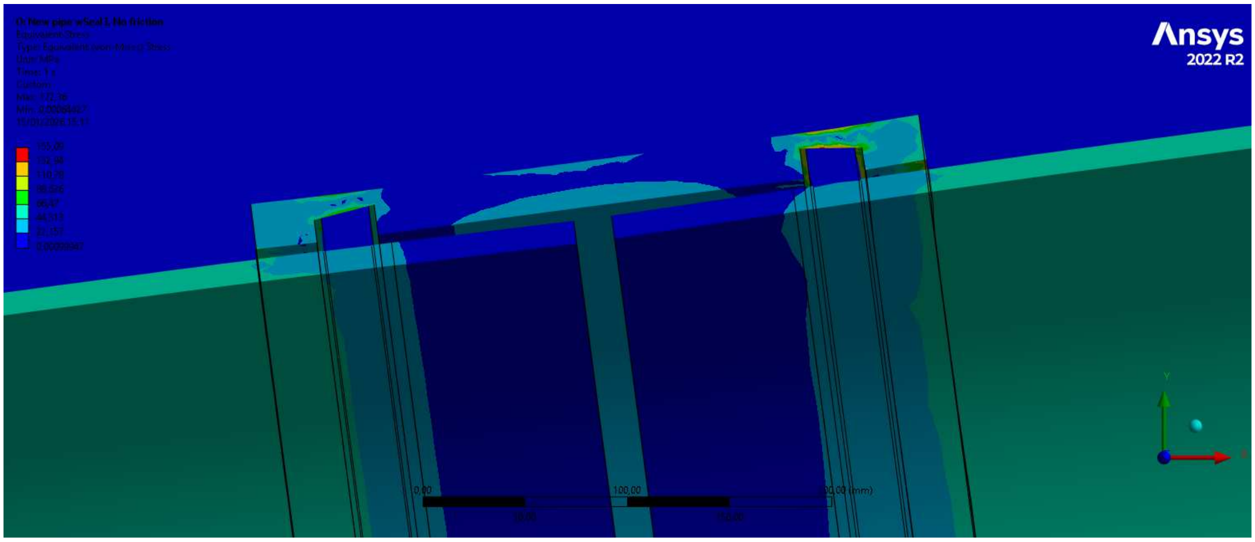

Figure 12 Von-mises stress coupler, gaskets and pipe ends

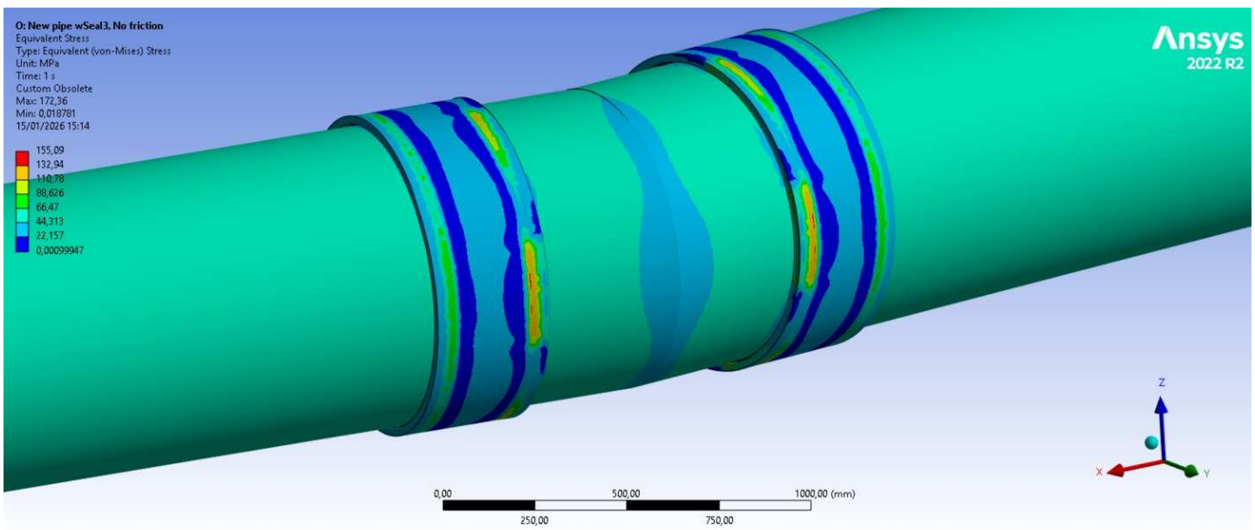

Figure 13 Von-mises stress external view of pipe bend

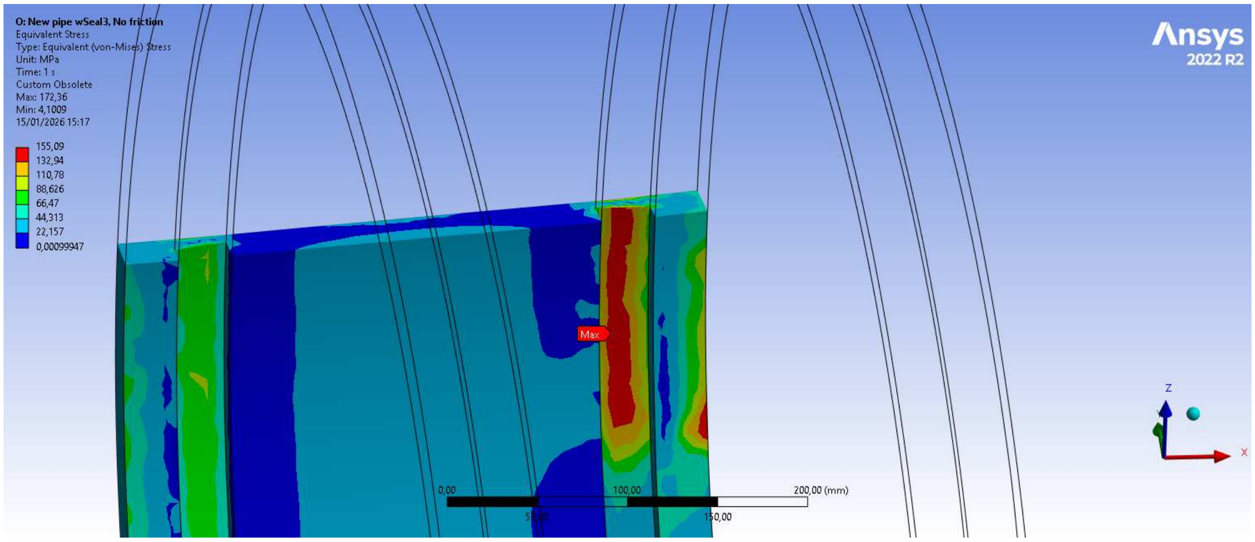

Figure 14 Von-mises stress hot spots within coupler behind gaskets

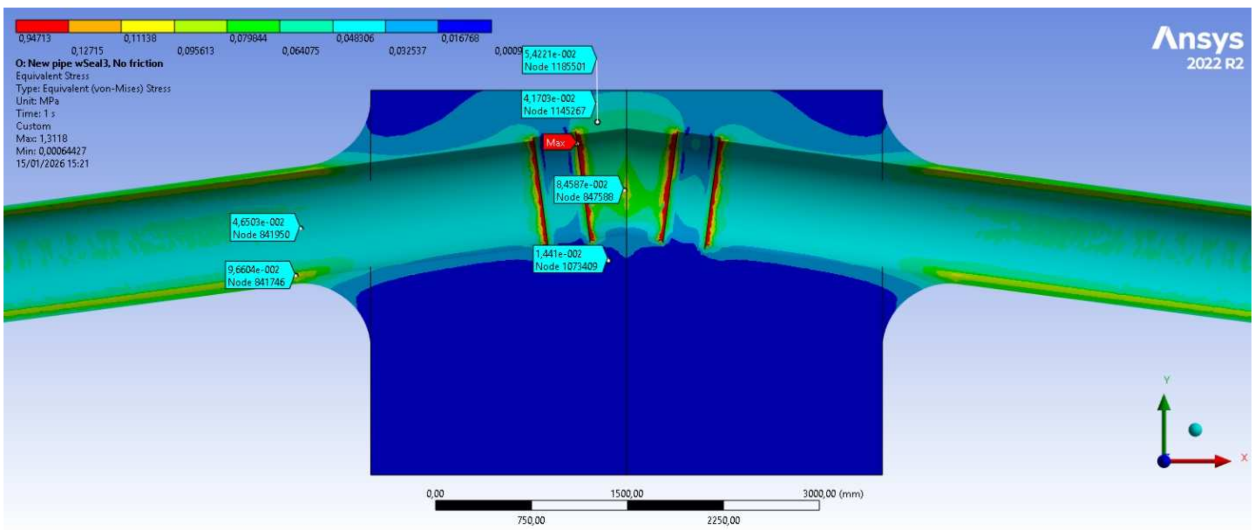

Figure 15 Von-mises stress of cross-sectional view with probe values

Pipe stresses (Axial, Hoop & Radial)

Axial

The axial stress shows high and negative hotspots near the foam boundary at the coupler. This due to stiffness change, supported and unsupported pipe segments.

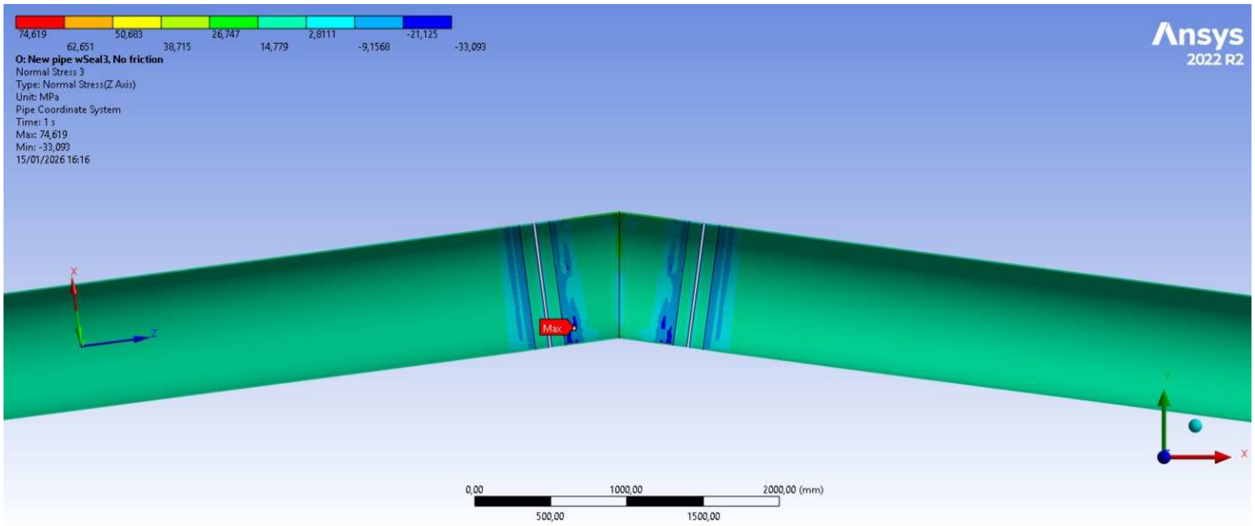

Figure 16 Pipe axial stress, cross-sectional view

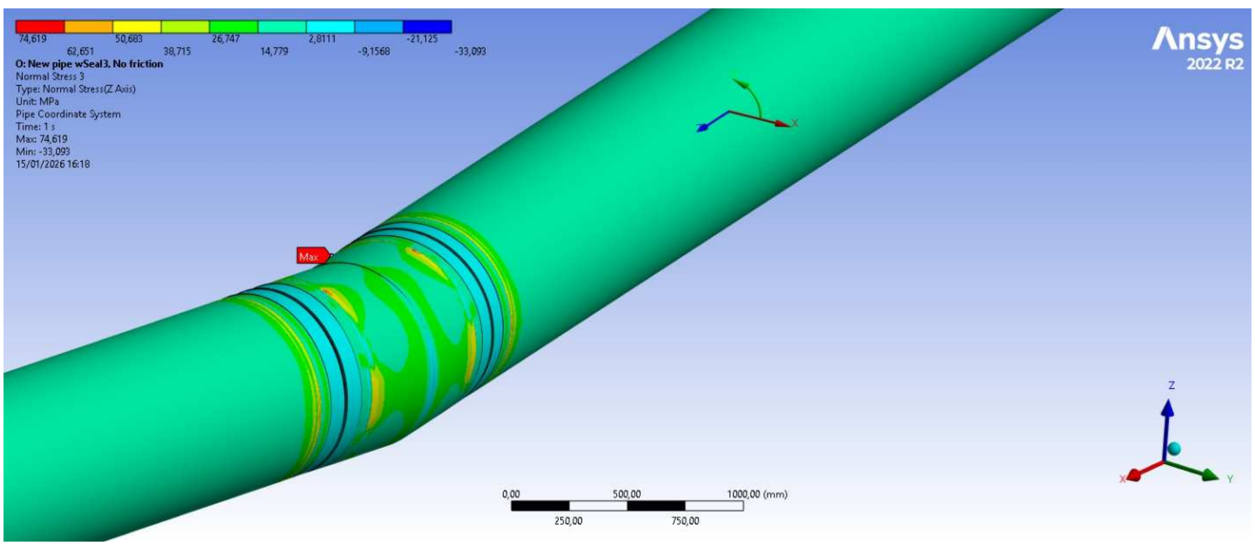

Figure 17 Pipe axial stress near the bend region, external view

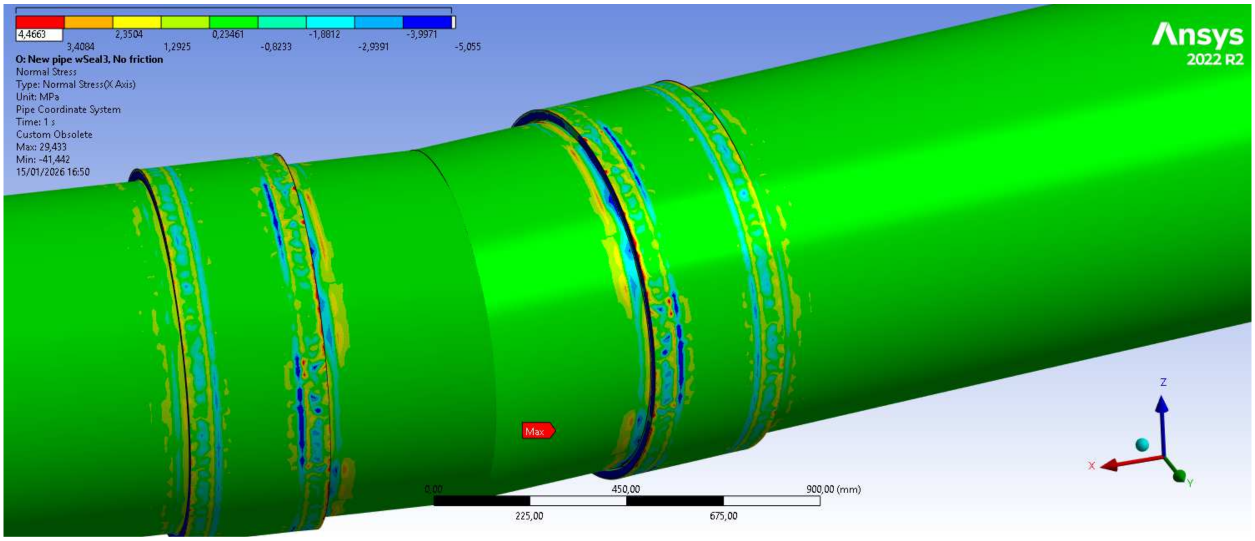

Figure 18 Pipe and coupler axial stress, external view

Hoop

The hoop stress is uniform within the pipe, however show exceptions at the pipe ends, this as counter water pressure is acting on either side of the pipe ends, within the coupler gaskets bounds.

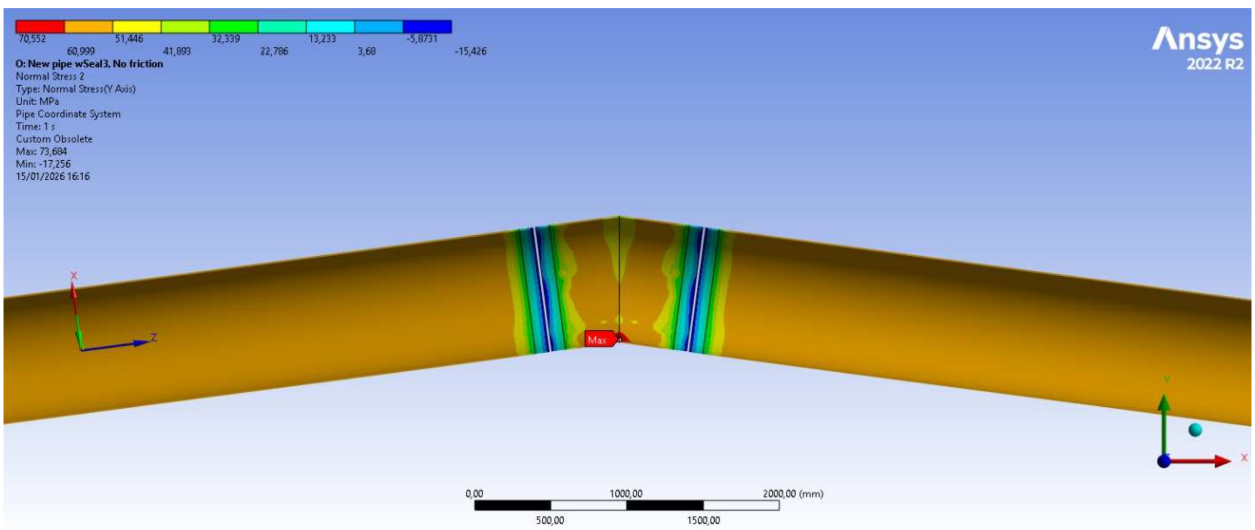

Figure 19 Pipe hoop stress, cross-sectional view

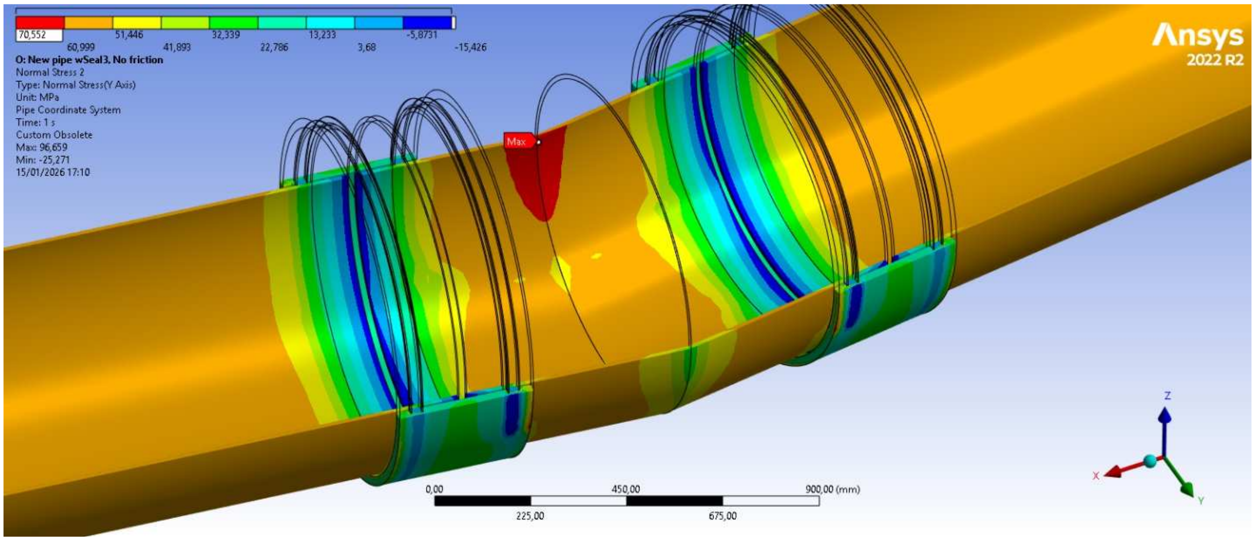

Figure 20 Pipe and coupler hoop stress cross-sectional view, close up.

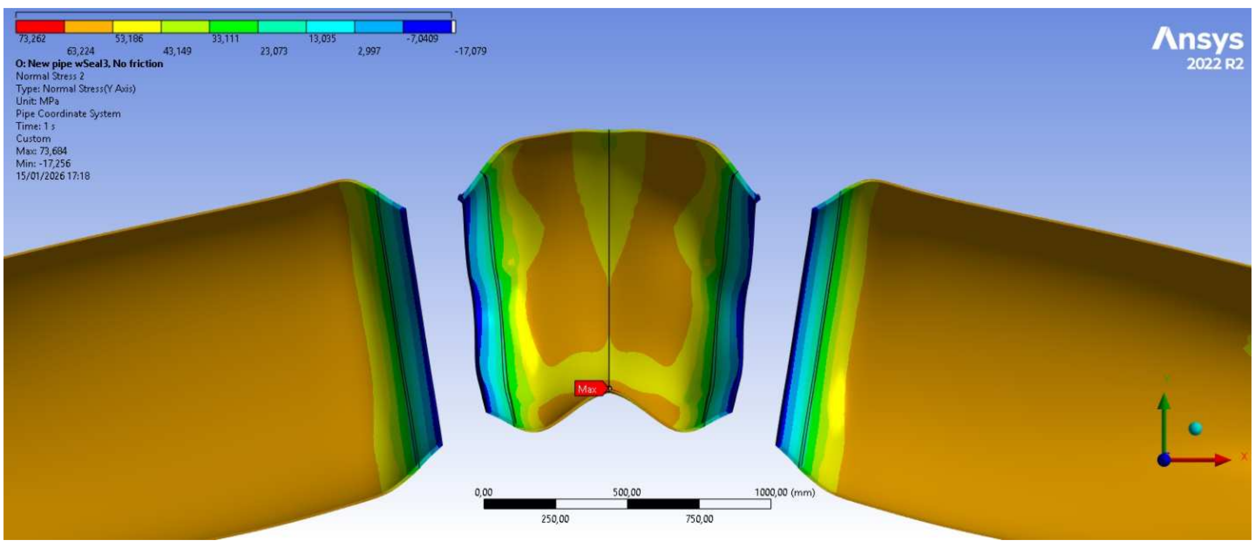

Figure 21 Pipe hoop stress near bend region, 33x deformation scale close up of bend

This highly deformation representation clearly indicates why the hoop stresses are higher or lower in certain areas.

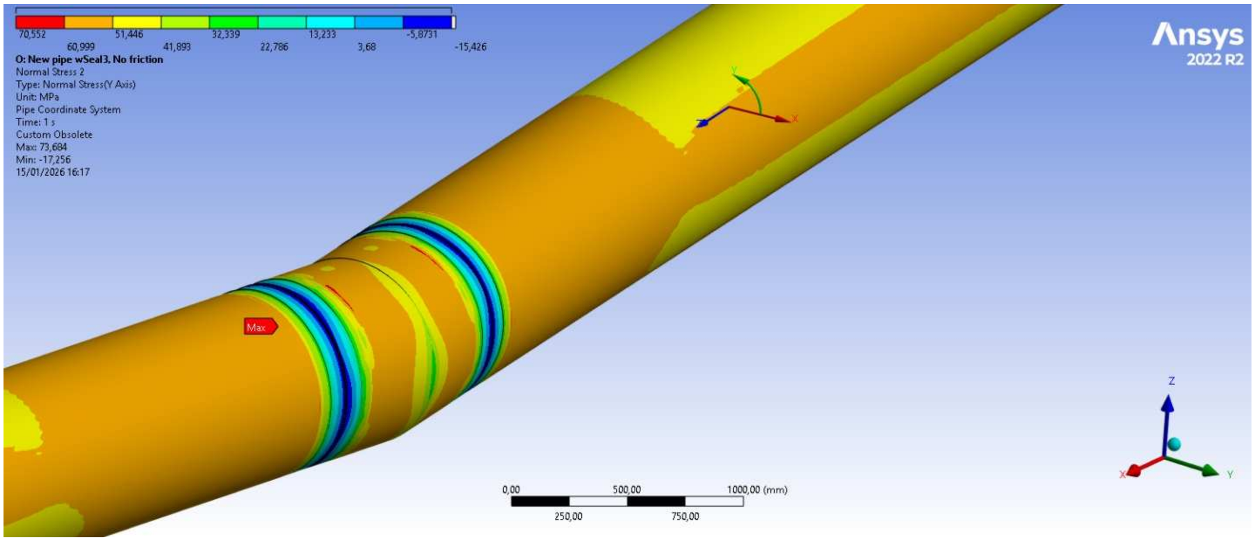

Figure 22 Pipe hoop stress of bend, 1x deformation, external view

Radial

The radial stress in the pipe wall is generally low along most of the pipe length, with localized variations near the coupler and pipe ends. In the main pipe section, internal pressure acts on the inner wall, causing uniform outward expansion. Near the pipe ends, this deformation is restricted by the coupler, foam, and surrounding soil, which alters the stress distribution.

This restraint limits circumferential expansion, leading to local compressive stresses, ovalisation, and localized shell instability (wrinkling) at the pipe–coupler interface. As a result, stress concentrations develop in these regions due to the reduced deformation capacity of the pipe ends.

The scope of this simulation is not focused on the gasket / sealing application. Therefore, these results on the pipe end might vary with real-life results. Also, the usage between different type of gaskets will be of influence.

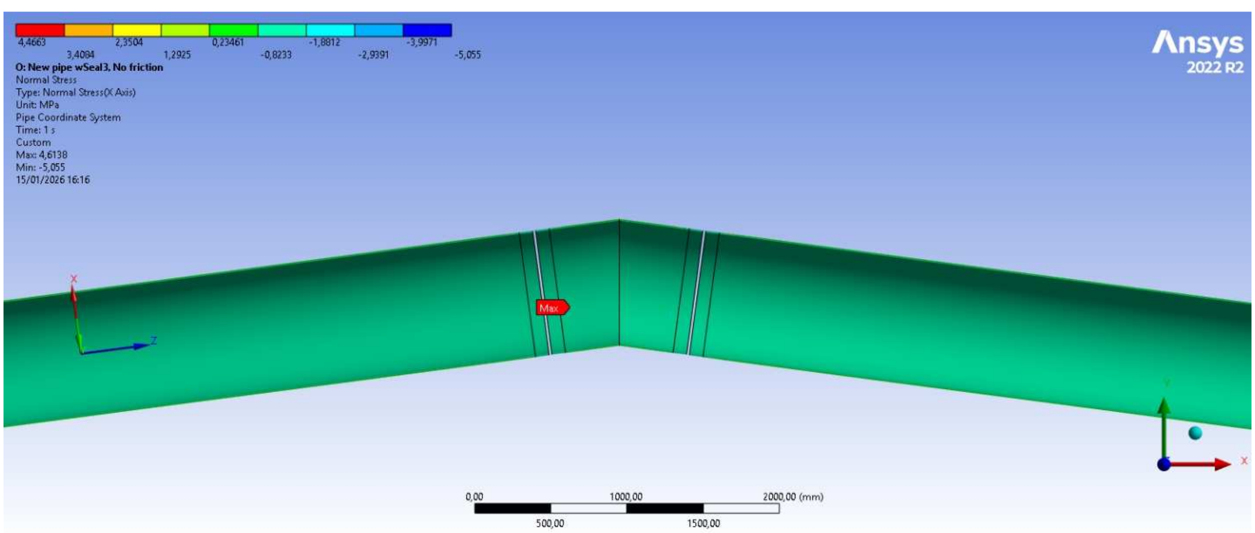

Figure 23 Pipe radial stress, cross-sectional view

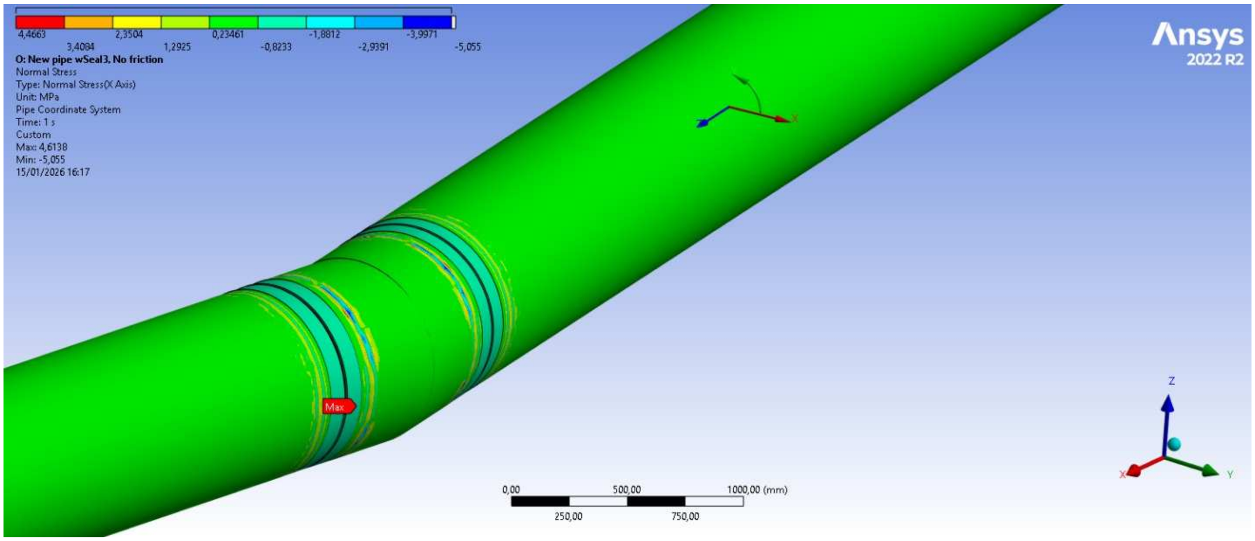

Figure 24 Pipe radial stress, external view

Pipe Y-deformation (bend direction)

One of the main deformation responses as a result of the internal pressure is the Y- deformation in the direction of the bend apex. A maximum of ~5mm has been measured near the bend apex. Besides this measurement a smooth distribution is seen throughout the pipe. This Y-deformation is a combination of pipe displacement in the Y-direction and pipe circumferential deformation due to the pipe internal stresses.

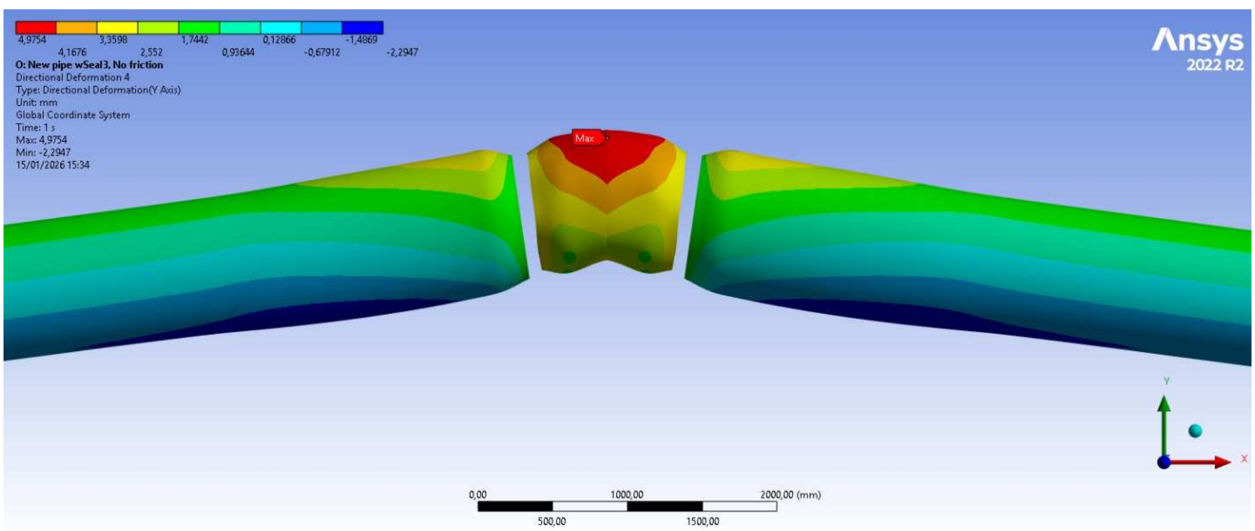

Figure 25 Y-deformation, 33x deformation scale, top view

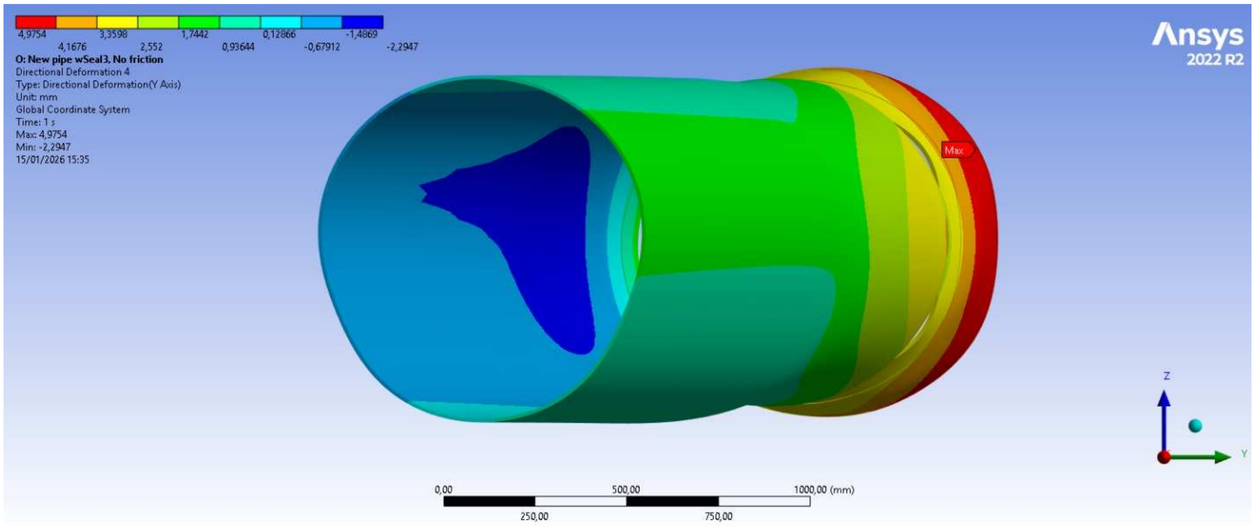

Figure 26 Y-deformation, 33x deformation scale, side view

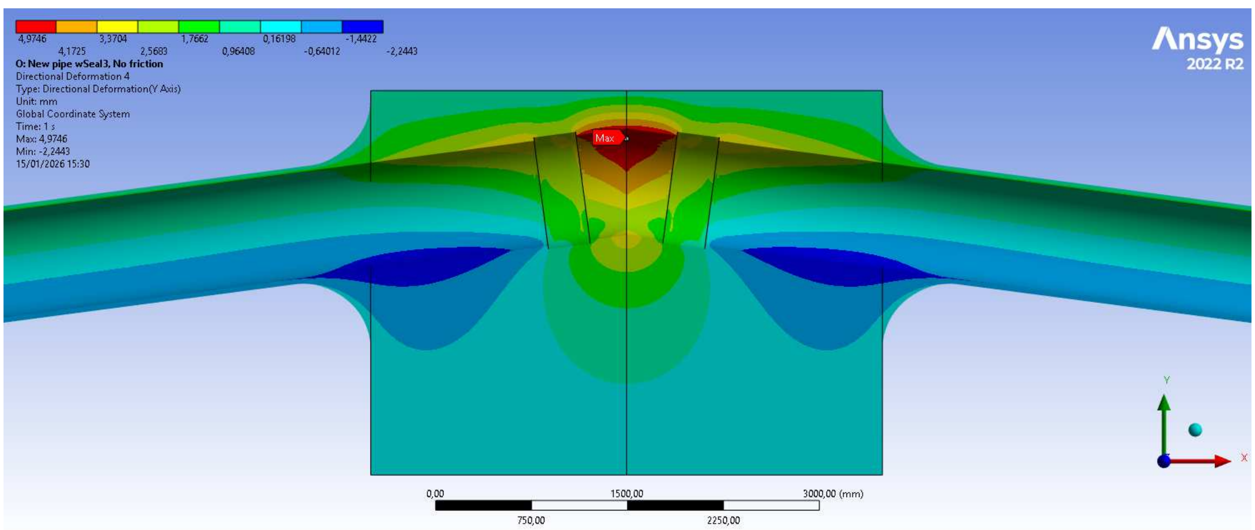

Figure 27 Y-axis deformation within foam, cross-sectional top view

Compressive strain foam

The minimum principle elastic strain will give a good indication of how the foam is being compressed. With the blue color indicating the highest compressed area.

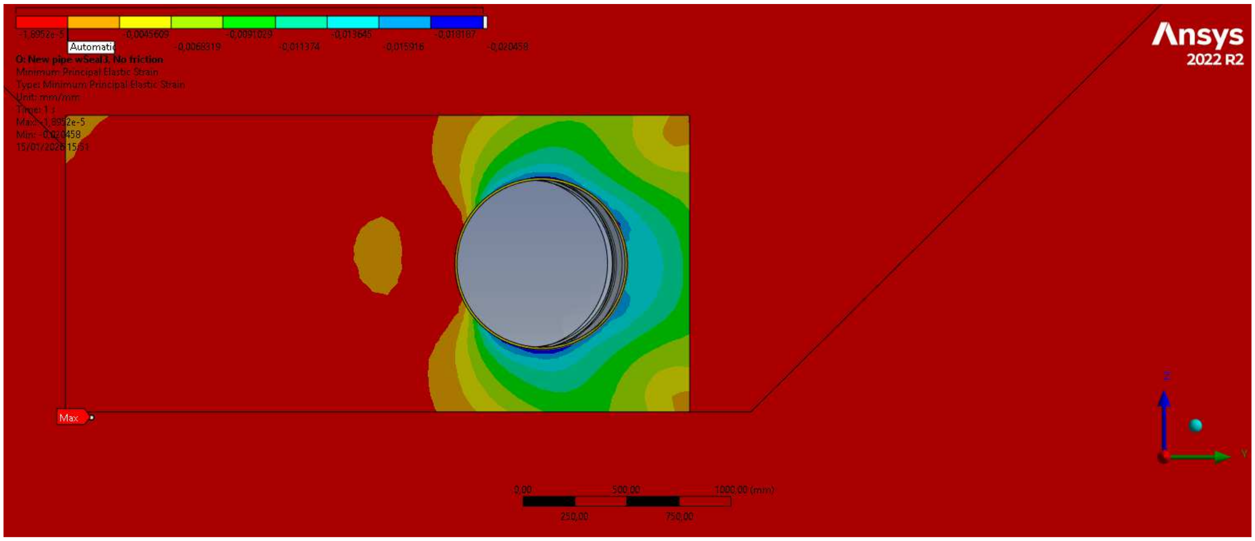

Figure 28 Minimum principle elastic strain (2D symmetry plane)

Compressive stress foam, backfill and insitu-soil

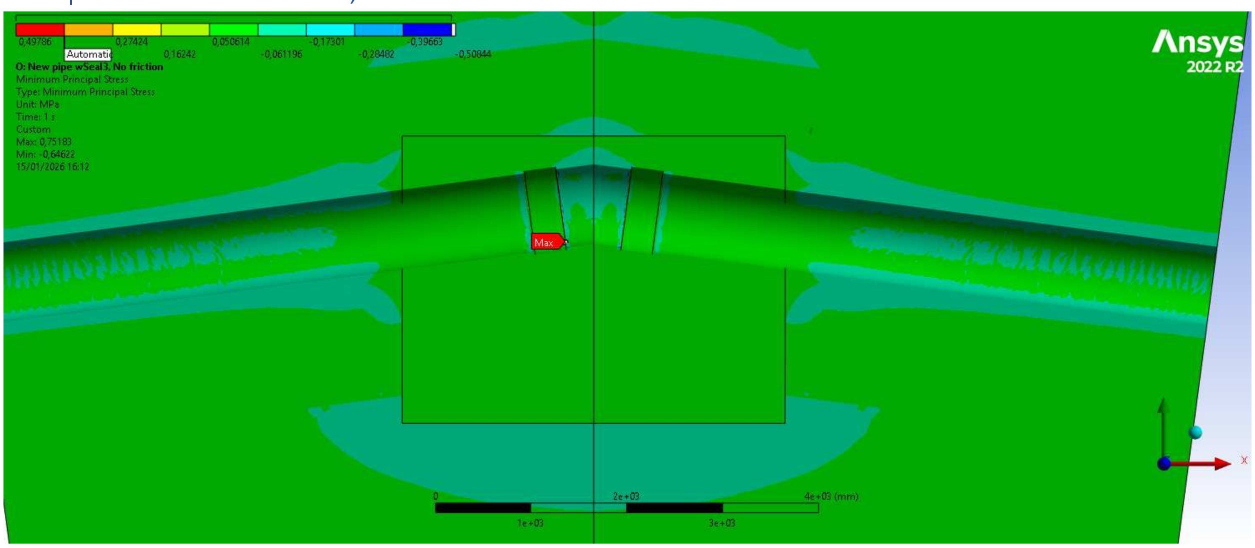

Figure 29 Minimum principle stress

Tensional strain foam

The maximum principle elastic strain will give a good indication of how the foam is being elongated. With the red color indicating the highest tensile strained area.

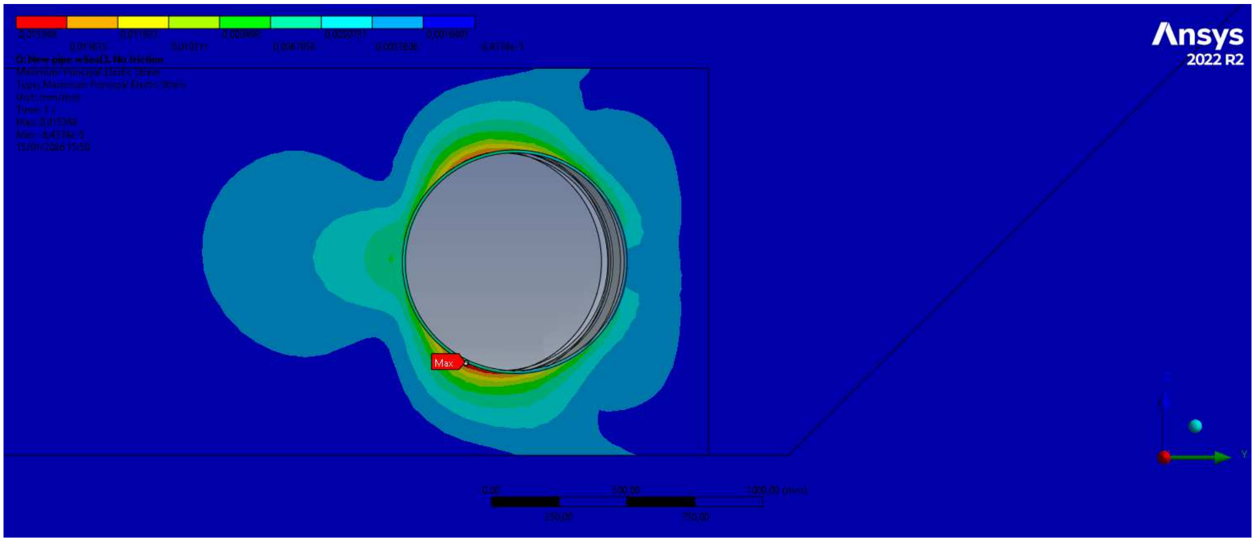

Figure 30 Maximum principle elastic strain (2D symmetry plane)

Tension stress foam, backfill and insitu-soil

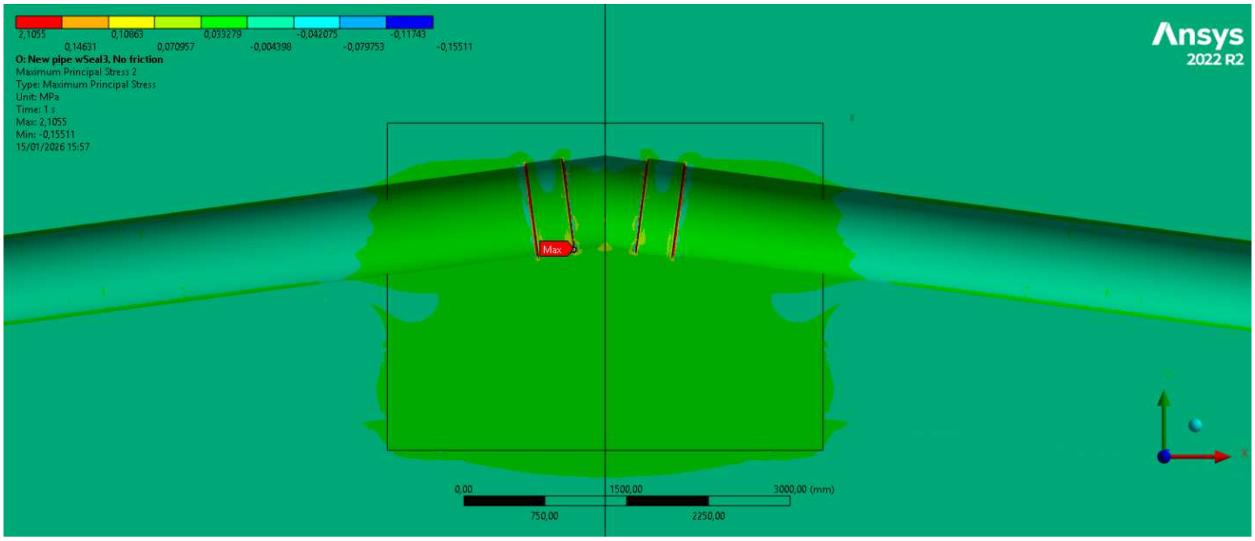

Figure 31 Maximum principle stress, cross-sectional top view

Total strain foam

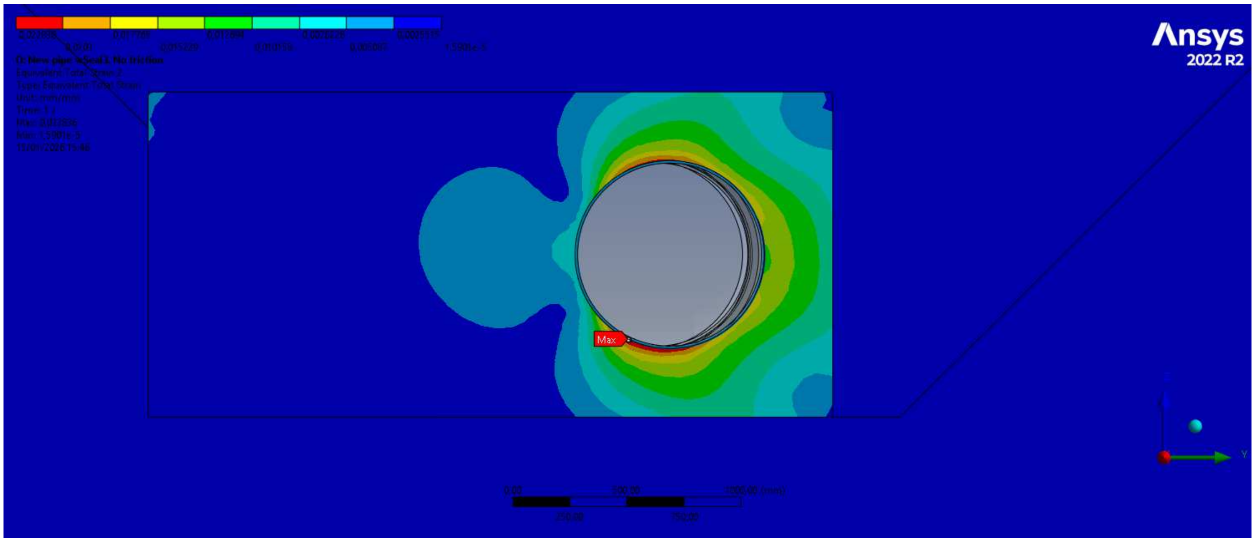

Figure 32 Total strain (2D symmetry plane)

Misalignment, deflection & retraction of pipe ends

The misalignment angle between the straight pipe segment and the bend pipe segment is evaluated within the coupler to assess joint alignment under the applied loading conditions. In addition, the center-point misalignment distance between the pipe ends is measured to quantify relative lateral displacement within the coupler.

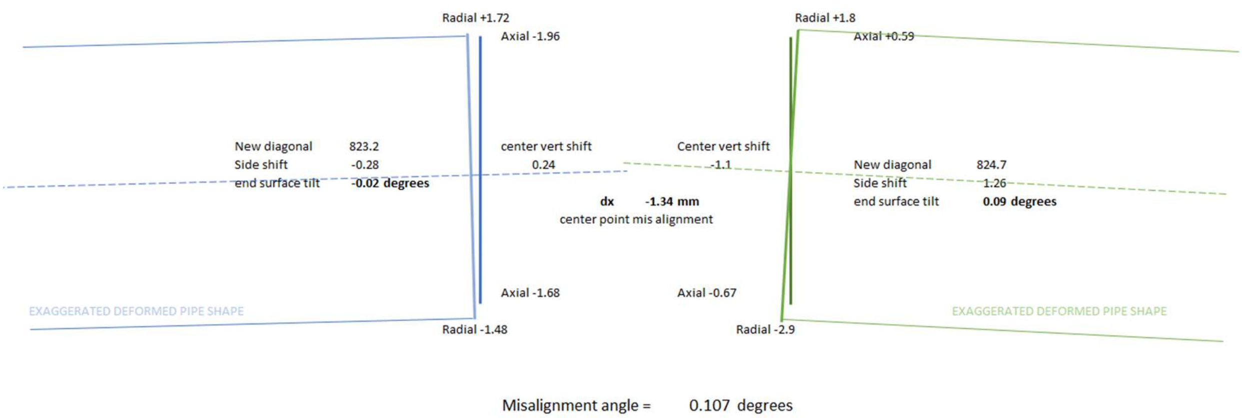

Figure 33 Pipe ends mis-alignment and displacement

A mis-alignment angle of 0.1 degree and center point displacement of -1.3 mm is calculated.

Ovalization of pipe at symmetry plane

To quantify pipe ovalization at the bend symmetry plane, four probe points are defined on the pipe cross-section at 0°, 90°, 180°, and 270° locations. These probe points measure the local Y-direction and Z-direction displacements on the 2D symmetry surface. By comparing the relative displacement of opposing points, changes in the effective pipe diameters in both the Y and Z directions can be determined, allowing the degree of ovality to be evaluated independently from global pipe translation.

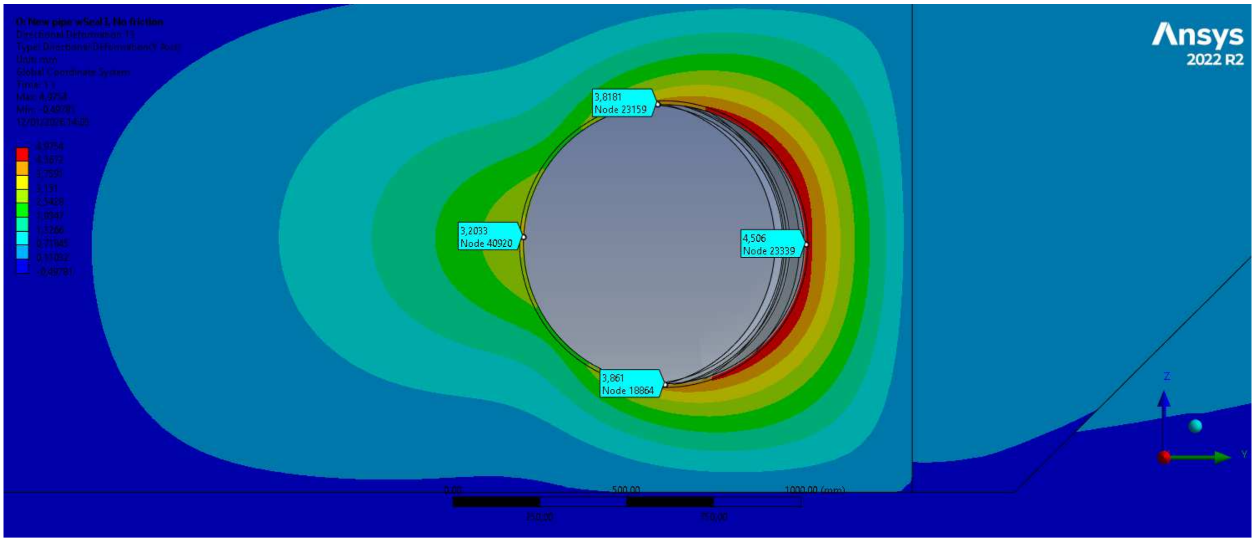

Figure 34 Pipe bend cross-sectional Y-axis deformation (2D symmetry plane)

By subtracting mean measurement at 0° and 180° from the apex(90°) and intrados(270°), we get the Y-deformation values at the intrados (3.2-3.8=-0.6mm) and apex (4.5-3.8=0.7mm).

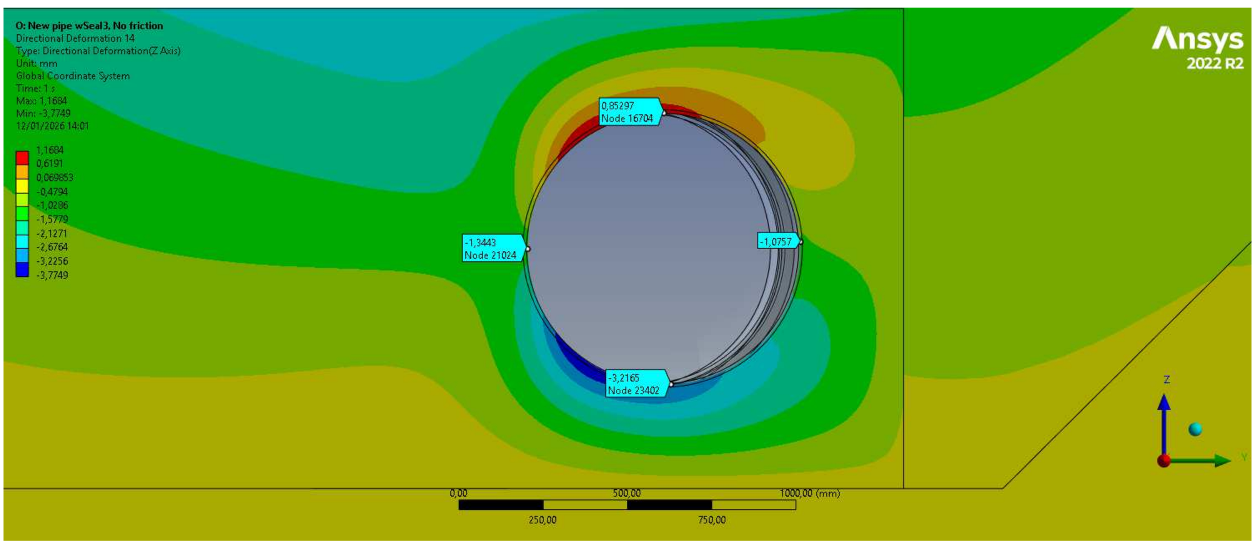

Figure 35 Pipe bend cross sectional Z-axis deformation (2D symmetry plane)

Similar for the Z-displacement. By subtracting mean measurement at apex(90°) and intrados(270°) from the 0° (top pipe) and 180° (bottom pipe), we get an indication of the local Z-deformation values at the top of the pipe (0.85+1.2=2.05mm) and bottom of the pipe (-3.2+1.2=-2mm). These measured values are the local deformation values, not the total deformation that also accounts for displacement

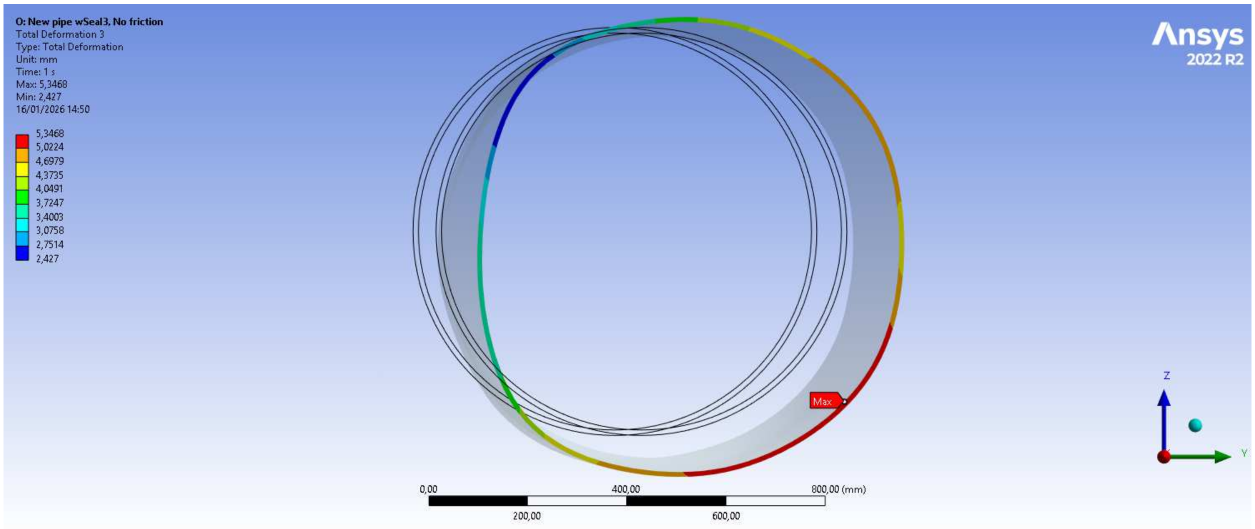

Figure 36 Pipe bend cross sectional deformation (2D symmetry plane), 26x deformation scale

26x deformation scale of the 2D pipe section on the symmetry plane shows the pipe over exaggerated total deformation.

Reaction forces

Reaction forces are obtained from the fixed supports and displacement boundaries in the model. Because a symmetry condition is applied at the mid-plane of the 15° bend, the calculated Y- and Z-direction reaction forces represent only half of the physical system and therefore must be multiplied by two to obtain the total forces for the full pipeline. The X-direction forces on the symmetry plane cancel out by symmetry and do not contribute to the global reaction force. All reported reaction forces are interpreted based on these considerations.

Object Name	*Force Reaction*	*Force Reaction 2*
State	Solved	
Definition		
Type	Force Reaction	
Location Method	Boundary Condition	
Boundary Condition	Fixed Support	Displacement
Orientation	Global Coordinate System	
Suppressed	No	
Options		
Result Selection	All	
Display Time	End Time	
Results		
X Axis	9178,9 N	3,1456e+005 N

Y Axis	-1,3784e+005 N	41381 N
Z Axis	5,7632e+006 N	81519 N
Total	5,7649e+006 N	3,2757e+005 N
Maximum Value Over Time		
X Axis	9178,9 N	3,1456e+005 N
Y Axis	-1,3784e+005 N	41381 N
Z Axis	5,7632e+006 N	81519 N
Total	5,7649e+006 N	3,2757e+005 N
Minimum Value Over Time		
X Axis	9178,9 N	3,1456e+005 N
Y Axis	-1,3784e+005 N	41381 N
Z Axis	5,7632e+006 N	81519 N
Total	5,7649e+006 N	3,2757e+005 N

Conclusion

The numerical analysis of the DN800 pipeline with a 15° buried bend demonstrates a stable and well-restrained structural response under the applied loading conditions. The results show minimal total deformation at the bend apex, with a maximum displacement of approximately 5 mm, indicating effective load transfer and confinement by the surrounding foam and soil. Deformation is well distributed through the foam block, confirming its ability to retain the pipe system and reduce localized stress concentrations.

Pipe end deformation and misalignment within the coupler are observed to be very small, suggesting that the current configuration provides adequate structural continuity between the straight and bend pipe segments. Overall, the results indicate that the pipeline system performs satisfactorily for the assessed load case, with no indications of excessive deformation or instability.

Recommendation

The current simulation was primarily focused on evaluating the global deformation behavior of the pipe bend system. While the overall results are satisfactory, the stiffness representation and gasket properties have been simplified, limiting the ability to assess detailed gasket behavior and localized coupler stresses. For a more comprehensive evaluation, it is recommended that a more refined FEM model is to be developed, incorporating detailed gasket geometry, material nonlinearity, and contact behavior.

Such an enhanced model would allow for improved prediction of gasket response, sealing performance, and stress distribution within the coupler. This level of detail is necessary should gasket integrity or coupler stress limits become governing design considerations.

Appendix

A-Convergence

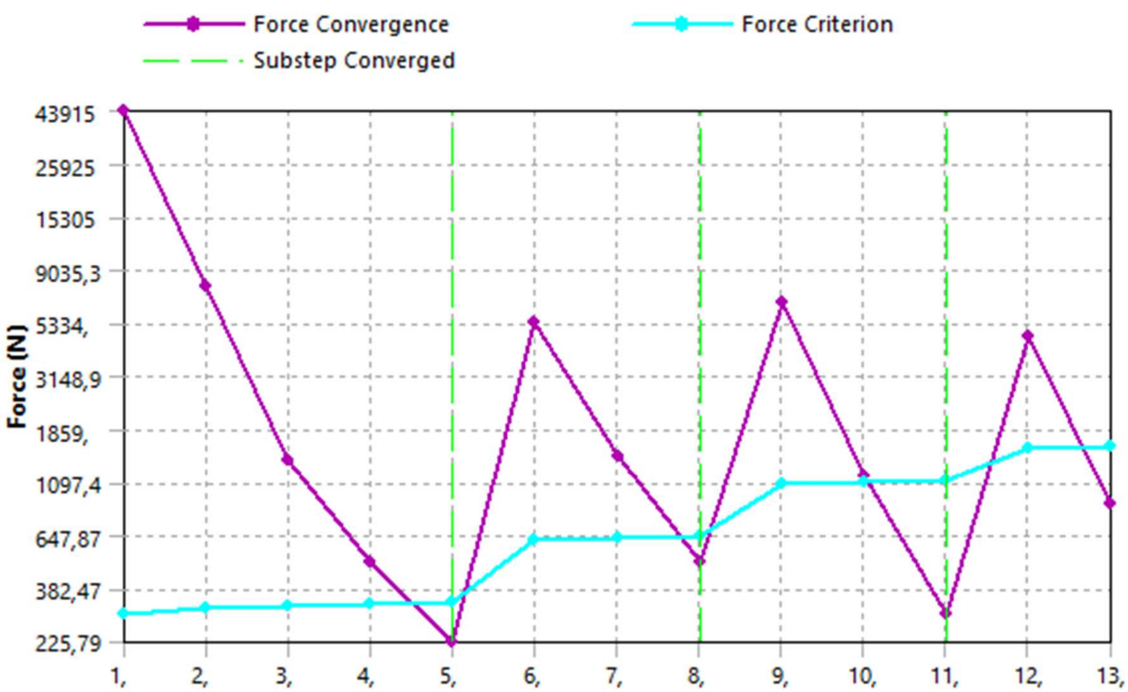

Appendix 1 Force convergence solution information

B- Cumulative iterations

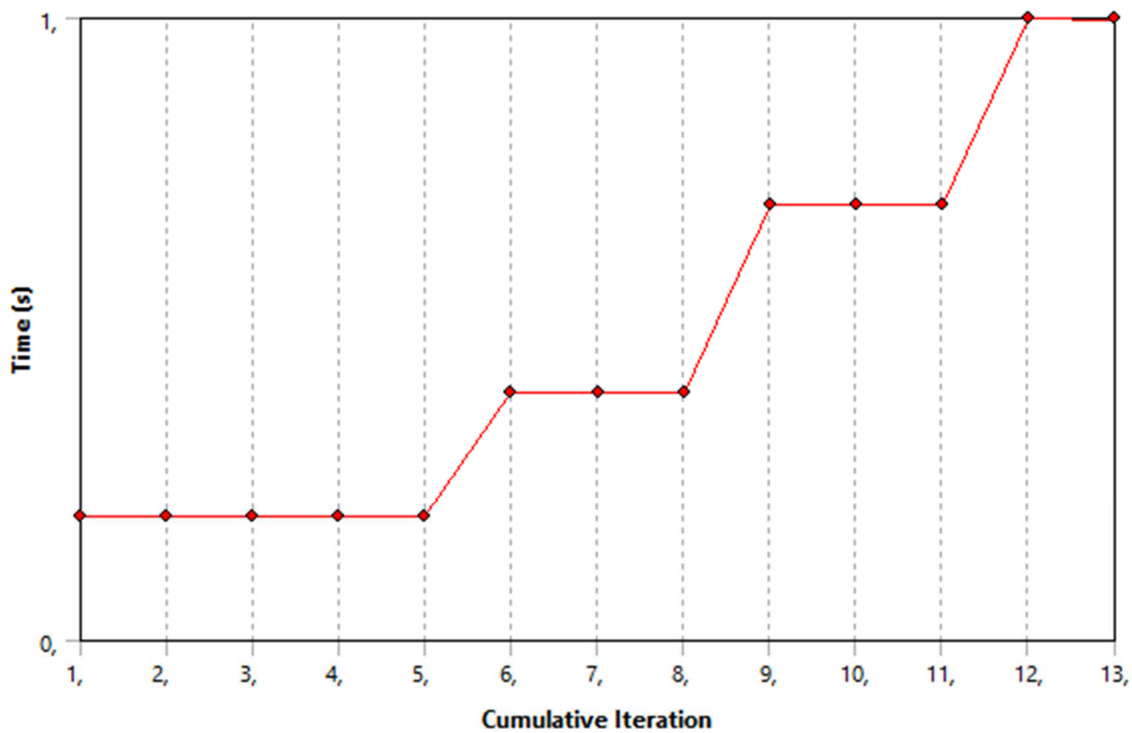

Appendix 2 Cumulative Iteration pseudo time

C-Additional gasket comparison

Additional simulation Y-deformation results are compared. The comparison layout; top (no gasket), middle a 4MPa gasket and bottom an 8MPa gasket.

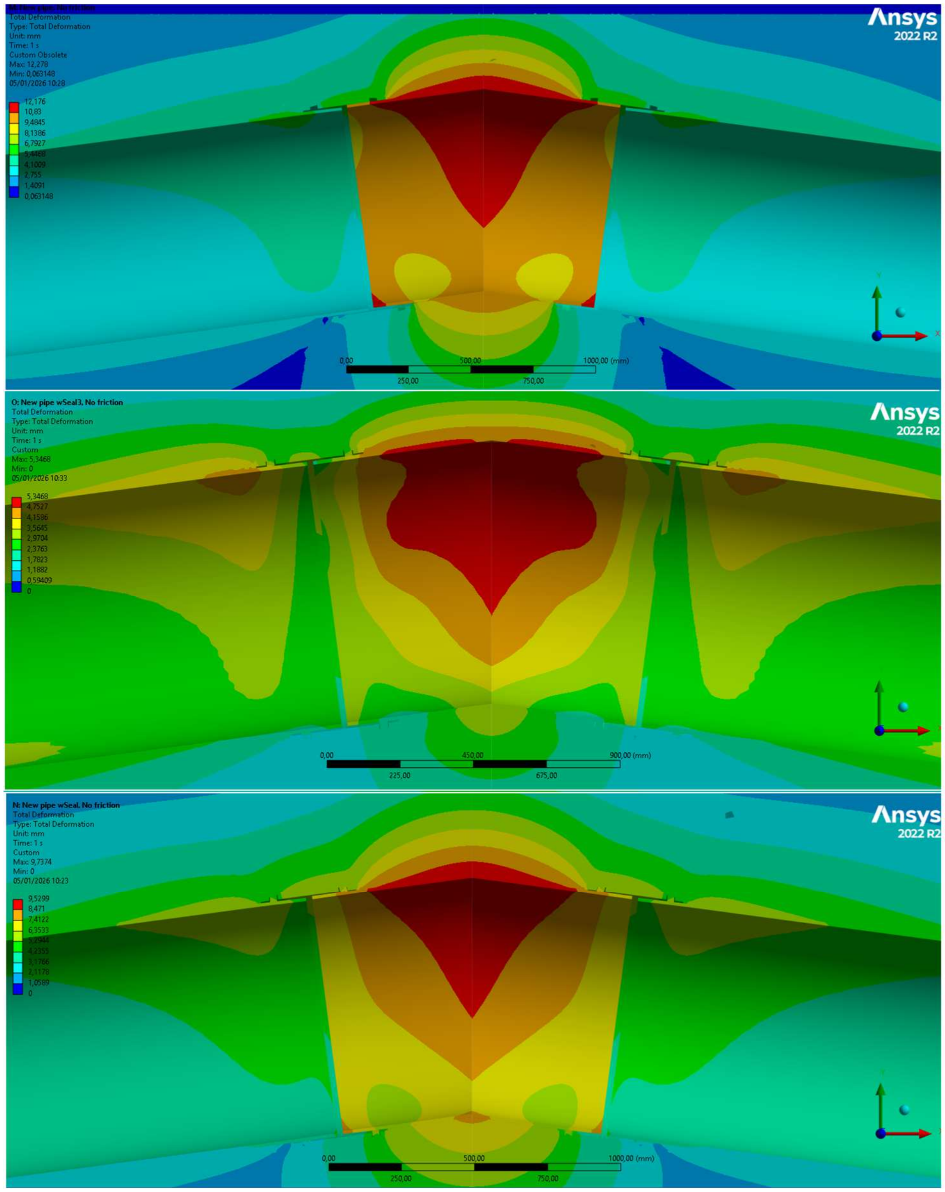

NO SEAL!
ALL FORCE IS ABSORBED BY FOAM.

RESULTS:
-HIGH DISPLACEMENT
-FULL BEND SECTION DISPLACEMENT
-BEND SECTION NOT ACTING ON COUPLER

4MPA SEAL
SEAL ELASTICITY CLOSE TO FOAM ELASTICITY

RESULTS:
-LOW DISPLACEMENT
-WELL DISTRIBUTED FORCES
-LESS LOCAL DEFORMATION IN PIPE BEND

8MPA SEAL
SEAL ELASTICITY HIGHER THAN FOAM ELASTICITY

RESULTS:
-COUPLER RECEIVES HIGHER FORCE
-AVERAGE DISPLACEMENT
-POOR DISTRIBUTION OF FORCES
-MORE LOCAL DEFORMATION IN PIPE BEND DUE TO HIGHER PIPE RESISTANCE BY SEAL

Appendix 3 Anchor data

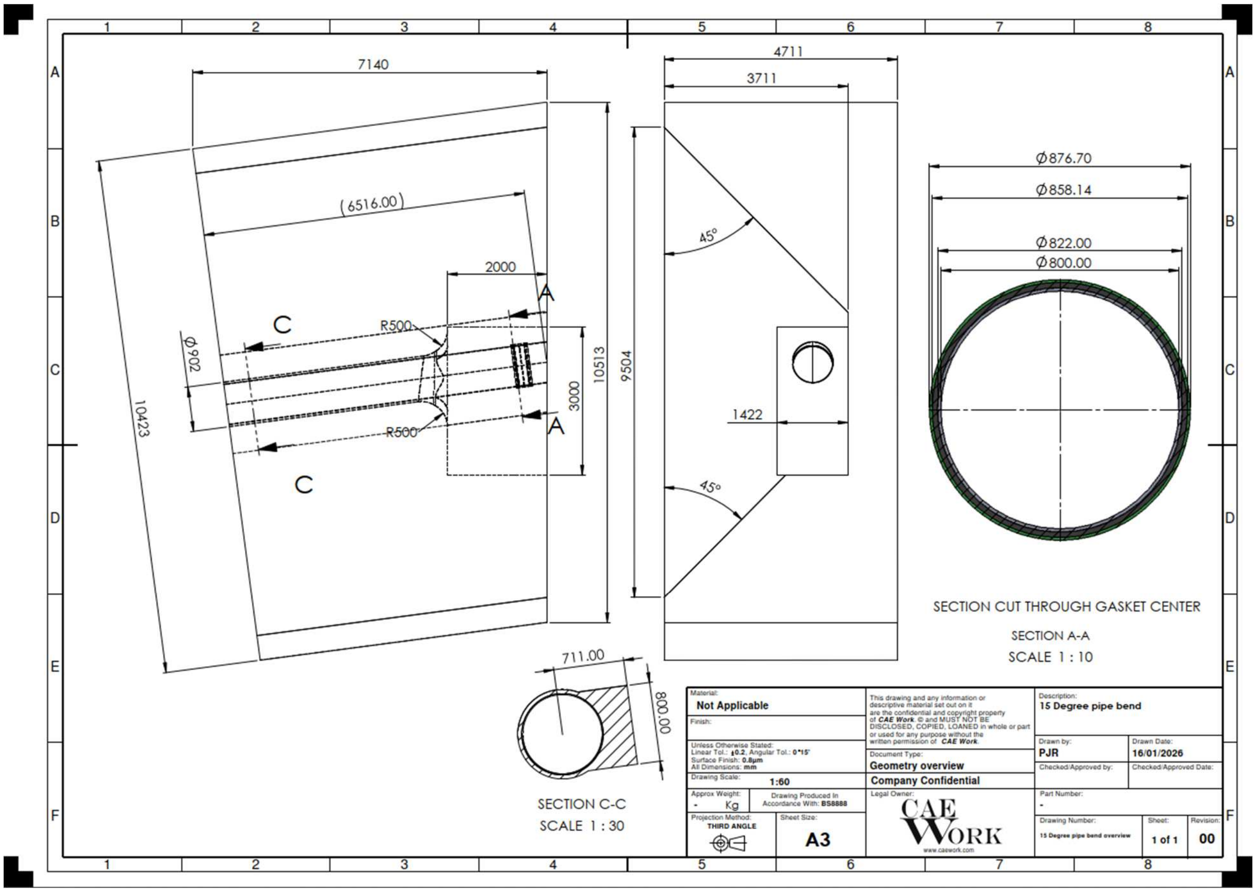

Appendix 4 Geometry drawing